# Design of Co-crystals/Salts of Aminopyrimidines and Carboxylic Acids through Recurrently Occurring Synthons

Samuel Ebenezer and P. Thomas Muthiah*

School of Chemistry, Bharathidasan University, Tiruchirappalli-620 024, India

Ⓢ *Supporting Information*

ABSTRACT: Fourteen crystals involving various substituted organic acid molecules and 2-amino-4,6-dimethylpyrimidine (MP)/2-amino-4,6-dimethoxypyrimidine (MOP) were prepared and characterized by using single crystal X-ray diffraction. Among the 14 crystals, proton transfer from the carboxylic acid to pyrimidine base has occurred only in 5 crystals while the remaining were co-crystals. It is obvious that the $R_2^2(8)$ ring motif occurs in co-crystals/salts when an acid interacts with a pyrimidine base. The present work has been focused on this aspect, confining the study to MP and MOP, where the results surely indicate that there are three main synthons, which regularly occur, linear heterotetramer (LHT), cyclic heterotetramer (CHT), and heterotrimer (HT). Among the whole lot, in both the present study and the literature, LHT is dominant as it occurs in 30 out of the existing 54 structures, while CHT and HT correspond to 9 each with the remaining structures forming newer synthons. Our results are also consistent with a recent paper in *Crystal Growth and Design* (**2008**, *8*, 4031−4044), where LHT is predicted to be more stable among other synthons. Furthermore in the present study, attempts have been made to correlate the formation of salts/co-crystals using ΔpK_a for both MP and MOP molecular complexes. The failure to explain MOP using ΔpK_a also suggests that the use of Pk_a values in predicting co-crystals/salts could vary from system to system.

LHT- Linear heterotetramer HT- Heterotrimer CHT-Cyclic heterotetramer
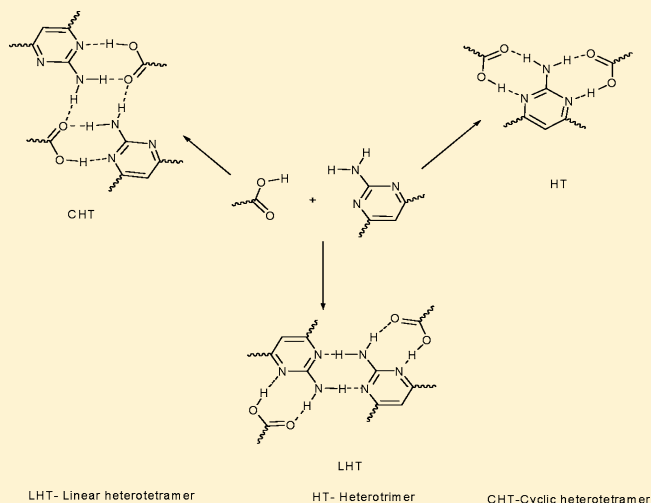
INTRODUCTION

Numerous organic molecular motifs form the essential structural components of biological systems and drugs. The three-dimensional structures and interaction of bioorganic motifs are of immense importance in the existence of biological systems and in molecular recognition. Molecular recognition refers to the selective binding of two or more molecules through noncovalent interactions such as hydrogen bonding, hydrophobic forces, van der Waals forces, $\pi-\pi$ interactions and electrostatic forces.[1] They play a very important role in biological systems as demonstrated in antigen−antibody, DNA−protein, sugar−lectin, and many other interactions.[2−6] They are also vital parts of many biochemical processes such as enzyme action, molecular transport, genetic information transfer and protein assembly.[7,8]

From the perspective of crystal engineering, a detailed understanding of the supramolecular chemistry of functional groups in a compound is prerequisite for rationally designing salts and co-crystals with desired structural features. The key to this has been the identification of the recurrently occurring supramolecular synthons. Use of synthetic strategies such as hydrogen bonding, halogen bonding, and stacking interactions have been very common in building these synthons and

among the whole lot, hydrogen bonding has been more prevalent because of its strength, directionality, and predictability.[9−13] Homosynthons and heterosynthons are the two distinctively categorized types of synthons.[14,15] The preference in the formation of supramolecular heterosynthons over homosynthons is evident from the large number of reports in the literature.[16−21] Moreover in the context of the present study it is very clear from the systematic analysis of the bimolecular ring motifs in organic crystal structures that the occurrence of supramolecular heterosynthons (2-substituted nitrogen heterocyclic system with carboylic acid group) are statistically high when compared to the individual homosynthons.[22,23] More specifically in the present study we focus herein upon the ability of carboxylic acids to form other reliable and stable supramolecular heterosynthons with the pyrimidine derivatives.

Pyrimidines and aminopyrimidine derivatives are biologically important compounds and they manifest themselves in nature as components of nucleic acids. The functions of nucleic acids are explicitly determined by hydrogen bonding

Scheme 1. Molecular Components of Different Co-crystals and Salts
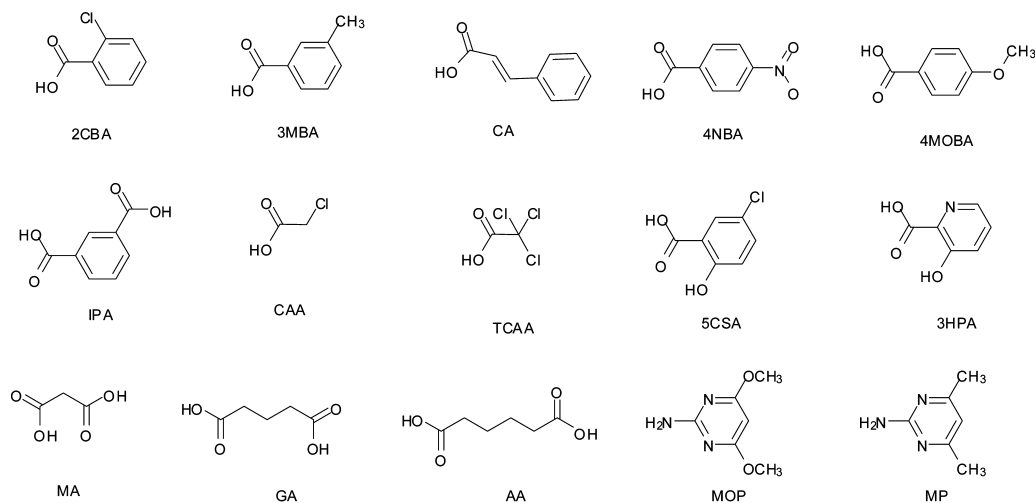
2CBA = 2-chlorobenzoic acid	3MBA = 3-methylbenzoic acid	CA = cinnamic acid	**1.** MOP.2CBA (1:1)
4NBA - 4-nitrobenzoic acid	4MOBA = 4-methoxybenzoic acid	IPA = isophthalic acid	**2.** MOP.3MBA (1:1)
CAA = chloroacetic acid	TCAA = trichloroacetic acid	5CSA = 5-chlorosalicylic acid	**3.** MOP.CA (1:1)
3HPA = 3-hydroxypicolinic acid	MA = malonic acid	GA = glutaric acid	**4.** MOP.4NBA (1:1)
AA = adipic acid	MOP = 2-amino-4,6-dimethoxypyrimidine	MP = 2-amino-4,6-dimethylpyrimidine	**5.** MOP.4MOB (1:1)

6. MOP.IPA (2:1)
7. MOP.CAA (1:1)
8. MOP$^+$.TCAA$^-$ (1:1)
9. MOP$^+$.5CSA$^-$ (1:1)
10. MOP$^+$.3HPA$^-$ (1:1)
11. MP$^+$.5CSA$^-$ (1:1)
12. MP$^+$.MA$^-$ (1:1)
13. MP.GA (2:1)
14. MP.AA (2:1)

patterns including base pairing which is responsible for genetic information transfer.[8,24] Aminopyrimidine derivatives also present themselves as the key components in many drugs.[25] Their interactions with carboxylic acids are of utmost importance since they are involved in protein−nucleic acid recognition and drug−protein recognition processes (where the pyrimidine moiety of a drug forms hydrogen bonding with the carboxyl group of the protein).[26−28] It is for this reason that the present work has been mainly focused on salts and co-crystals of aminopyrimidine derivatives (2-amino-4,6-dimethyl pyrimidine (MP) and 2-amino-4,6-dimethoxy pyrimidine (MOP)). Moreover in the recent years there has been massive interest in the co-crystals/salts involving Active Pharmaceutical Ingredients because of their applications in drug formulation.[29−32] Therefore to gain deep knowledge and understanding of a detailed supramolecular organization in the salts/co-crystals, carboxylic acids with different modifications have been tried and attempts have been made to identify their effect on the hydrogen-bonded supramolecular motifs. Scheme 1 shows the molecular structure of various carboxylic acids along with the pyrimidine derivatives which give rise to different salts and co-crystals. A large number of MP/MOP-carboxylate/carboxylic acid complexes has earlier been reported from our laboratory.[33−46]

■ EXPERIMENTAL SECTION

Compounds 1−10 were prepared by mixing hot methanolic solution of 2-amino-4,6-dimethoxypyrimidine with hot methanolic solution

of 2-chlorobenzoic acid/3-methylbenzoic acid/cinnamic acid/ 4-nitrobenzoic acid/4-methoxybenzoic acid/isophthalic acid/chloroacetic acid/trichloroacetic acid/5-chloro salicylic acid/3-hydroxy picolinic acid in 1:1 molar ratio and were allowed to warm over a water bath for half an hour. The mixtures were cooled slowly and kept at room temperature. After a few days, colorless prismatic crystals (for compounds 1, 3, 6, 9, and 10), colorless plate-like crystals (for compounds 2 and 5) and colorless needle-like crystals (for compounds 4, 7, and 8) separated out of the mother liquor.

Compounds 11, 12, and 14 were prepared by mixing hot methanolic solution of 2-amino-4,6-dimethylpyrimidine with hot methanolic solution of 5-chloro salicylic acid/malonic acid/adipic acid in 1:1 molar ratio and warmed in a water bath for few minutes. The mixtures were then allowed to cool slowly at room temperature. After a few days colorless needle-like crystals (for compound 11, 12, and 14) separated out of the mother liquor. Similarly compound 13 was prepared by mixing ethanolic solution of 2-amino-4,6-dimethylpyrimidine with hot ethanolic solution of glutaric acid in 1:1 molar ratio. It was allowed to warm over a water bath for half an hour and then left for slow evaporation at room temperature. After a few days, colorless plate-like crystals separated out of the mother liquor.

2-amino-4,6-dimethoxypyrimidine and 2-amino-4,6-dimethylpyrimidine were purchased from Sigma-Aldrich, Inc. Chloroacetic acid, cinnamic acid and glutaric acid were purchased from S.d. Fine chemicals Pvt. Ltd., India, whereas the rest of the acids were purchased from Loba chemie Pvt. Ltd., India.

■ X-RAY CRYSTALLOGRAPHY

Single crystal diffraction data for all crystal structures were collected on Bruker SMART APEX-II diffractometer equipped by a CCD-detector with graphite monochromated Mo Kα

Table 1. Crystallographic Table for Structures 1–14

	1	2	3	4	5	6	7
compound reference	MOP·2CBA	MOP·3MBA	MOP·CA	MOP·4NBA	MOP·4MOBA	MOP·IPA	MOP·CAA
chemical formula	$C_6H_9N_3O_2·C_7H_5ClO_2$	$C_6H_9N_3O_2·C_8H_8O_2$	$C_6H_9N_3O_2·C_7H_8O_2$	$C_6H_9N_3O_2·C_7H_5NO_4$	$C_6H_9N_3O_2·C_8H_8O_3$	$2(C_6H_9N_3O_2)·C_8H_6O_4$	$C_6H_9N_3O_2·C_3H_3ClO_2$
formula mass	311.72	291.31	303.32	322.28	307.31	476.45	249.66
crystal system	triclinic	triclinic	triclinic	monoclinic	monoclinic	triclinic	monoclinic
a (Å)	7.7162(3)	7.5478(2)	4.99690(10)	4.76200(10)	7.02950(10)	9.4556(2)	12.6481(2)
b (Å)	7.9195(3)	7.8842(2)	11.1131(2)	10.9490(2)	26.2951(4)	11.1124(3)	4.03740(10)
c (Å)	12.2788(5)	13.4987(3)	14.0377(3)	28.4995(6)	8.53710(10)	11.8799(3)	21.2104(4)
α (deg)	86.575(3)	88.995(2)	93.866(2)	90.00	90.00	83.595(2)	90.00
β (deg)	86.801(2)	75.052(2)	92.245(2)	90.455(2)	106.8150(10)	74.5320(10)	91.7390(10)
γ (deg)	71.148(2)	73.045(2)	97.287(2)	90.00	90.00	66.940(2)	90.00
unit cell volume (Å³)	708.29(5)	740.92(3)	770.58(3)	1485.89(5)	1510.54(4)	1106.90(5)	1082.62(4)
temp (K)	293(2)	293(2)	293(2)	293(2)	293(2)	293(2)	293(2)
space group	$P\bar{1}$	$P\bar{1}$	$P\bar{1}$	$P2_1/c$	$P2_1/c$	$P\bar{1}$	$P2_1/c$
no. of formula units per unit cell, Z	2	2	2	4	4	2	4
radiation type	Mo Kα	Mo Kα	Mo Kα	Mo Kα	Mo Kα	Mo Kα	Mo Kα
abs coeff (μ/mm^{-1})	0.289	0.097	0.097	0.116	0.104	0.112	0.357
no.reflns measured	16 307	18 029	15 150	11 462	21 719	20 497	12 964
no. independent reflns	4214	5105	3540	2362	3249	4648	3197
R_{int}	0.0309	0.0397	0.0467	0.0301	0.0306	0.0367	0.0377
final R_1 values ($I > 2\sigma(I)$)	0.0465	0.0593	0.0459	0.0402	0.0388	0.0415	0.0425
final $R_2(F^2)$ values ($I > 2\sigma(I)$)	0.1167	0.1457	0.1178	0.0971	0.1054	0.1089	0.0938
final R_1 values (all data)	0.0850	0.1592	0.0928	0.0634	0.0537	0.0615	0.0833
final $R_2(F^2)$ values (all data)	0.1373	0.1883	0.1521	0.1101	0.1172	0.1216	0.1121
GOF on F^2	1.019	1.006	0.995	1.039	1.041	1.033	1.017
CCDC number	829212	829218	829219	829220	829221	829222	829223

	8	9	10	11	12	13	14
compound reference	MOP⁺·TCAA⁻	MOP⁺·5CSA⁻	MOP⁺·3HPA⁻	MP⁺·5CSA⁻	MP⁺·MA⁻	MP·GA	MP·AA
chemical formula	$C_6H_{10}N_3O_2·C_2Cl_3O_2$	$C_6H_{10}N_3O_2·C_7H_4ClO_3$	$C_6H_{10}N_3O_2·C_6H_4NO_3$	$C_6H_{10}N_3·C_7H_4ClO_3$	$C_6H_{10}N_3O_2·C_3H_3O_4$	$2(C_6H_9N_3)·C_5H_8O_4$	$2(C_6H_9N_3)·C_6H_{10}O_4$
formula mass	318.54	327.72	294.27	295.72	227.22	378.43	392.46
crystal system	monoclinic	orthorhombic	triclinic	monoclinic	triclinic	orthorhombic	monoclinic
a (Å)	12.2675(2)	14.4255(2)	8.54700(10)	16.0278(4)	4.1106(2)	29.6875(11)	8.2625(3)
b (Å)	15.2303(2)	11.6661(2)	8.97980(10)	24.0006(6)	9.8487(5)	4.6937(2)	17.4876(5)
c (Å)	7.12170(10)	17.4006(2)	19.2710(3)	7.3516(2)	13.7524(7)	14.2292(6)	14.3439(5)
α (deg)	90.00	90.00	85.1580(10)	90.00	85.906(4)	90.00	90.00
β (deg)	97.7280(10)	90.00	88.6310(10)	92.297(2)	85.005(3)	90.00	93.532(2)
γ (deg)	90.00	90.00	65.5310(10)	90.00	80.131(3)	90.00	90.00
unit cell volume (Å³)	1318.52(3)	2928.34(7)	1341.31(3)	2825.72(13)	545.53(5)	1982.76(14)	2068.63(12)
temp (K)	293(2)	293(2)	293(2)	293(2)	293(2)	293(2)	293(2)
space group	$P2_1/c$	Pbca	$P\bar{1}$	$P2_1/c$	$P\bar{1}$	$Pca2_1$	$P2_1/c$
no. of formula units per unit cell, Z	4	8	4	8	2	4	4
radiation type	Mo Kα	Mo Kα	Mo Kα	Mo Kα	Mo Kα	Mo Kα	Mo Kα
abs coeff (μ/mm^{-1})	0.704	0.289	0.116	0.281	0.110	0.093	0.091
no.reflns measured	13 775	20 538	32 294	14 018	11 548	11 612	15 297

Table 1. continued

	8	9	10	11	12	13	14
no. independent reflns	2916	5049	8848	2401	2843	986	3286
R_{int}	0.0281	0.0327	0.0273	0.0542	0.0322	0.0461	0.0410
final R_1 values $(I > 2\sigma(I))$	0.0352	0.0484	0.0446	0.0399	0.0682	0.0376	0.0495
final $R_2(F^2)$ values $(I > 2\sigma(I))$	0.0814	0.1213	0.1230	0.0919	0.1900	0.1116	0.1272
final R_1 values (all data)	0.0516	0.0866	0.0732	0.0770	0.1002	0.0425	0.0802
final $R_2(F^2)$ values (all data)	0.0894	0.1390	0.1451	0.1109	0.2196	0.1160	0.1497
GOF on F^2	1.043	1.028	1.022	1.030	1.000	1.128	1.028
CCDC number	829224	829225	829213	829214	829215	829216	829217

radiation $(\lambda = 0.71073$ Å). Data reduction and cell refinement were carried out using Bruker SAINT and the necessary absorption corrections were performed by multiscan method using SADABS.[47] In all cases, the structures were solved in the WinGX suite of programs by direct methods using SHELXL-86/SHELXL-97 and refined using full-matrix least-squares techniques on F2 using SHELXS-97.[48] All non-hydrogen atoms were refined anisotropically and thereafter, all hydrogen atoms were placed in their geometrically idealized positions and constrained to ride on their parent atoms. Diagrams and publication material were generated using PLATON[49] and MERCURY.[50]

■ RESULTS

Crystallographic data for all the crystals are summarized in Table 1 and the hydrogen bonding parameters listed in Table 2. A detailed structural description of all the co-crystals and salts are given below in succession.

2-Amino-4,6-dimethoxypyrimidine-2-chlorobenzoic acid (1). The crystal structure of **1** crystallizes in triclinic space group, $P\bar{1}$, with a molecule of 2CBA and a molecule of MOP in the asymmetric unit. The main motif $(R_2^2(8))$ is assembled via a complementary hydrogen-bond interaction between the carboxylic acid and the amino-pyrimidine moiety to form a dimeric unit. Adjacent dimeric units are further connected through self-complementary secondary N−H···N hydrogen bonds to form a four-component supermolecule. Thus the primary and secondary hydrogen bonds, O−H···N, N−H···O, and N−H···N combine to form a linear heterotetramer motif. The supramolecular tetramer in **1** is planar and the adjacent tetramer supermolecules, produced from the weak hydrogen bonds, are connected into infinite 1-D tape via two symmetry related hydrogen bonds involving H8B of the methoxy group and O8 of another methoxy oxygen with both neighboring pyrimidine rings forming a ring motif through graph set notation $R_2^2(6)$ as shown in Figure 1 (symmetry codes $-x, 1 - y, 1 - z$). These tapes are interconnected to neighboring tapes through weak hydrogen bonds involving C12 of an acid ring and O7 of another methoxy group attached to the pyrimidine ring to form a supramolecular sheet (Figure 2) along (122) plane (symmetry codes $x, 1 + y, -1 + z$). Each layer of supramoleuclar sheets are stacked one with another through Π−Π stacking interactions. Stacking between the pyrimidine−pyrimidine and acid−acid rings are involved with centroid-to-centroid (Cg−Cg) distance of 3.5119(9) and 3.9200(12) Å and a slip angle (the angle between the centroid vector and the normal to the plane) of 11.79° and 23.68°, respectively.

2-Amino-4,6-dimethoxypyrimidine-3-methylbenzoic acid (2). 2 crystallizes in triclinic $P\bar{1}$ space group with the asymmetric unit possessing a molecule of MOP and 3MBA. The primary $R_2^2(8)$ motif connects the acid and amino-pyrimidine moiety to form a dimeric unit. A similar four component supermolecule is formed as in the previous case, through primary and secondary hydrogen bonds (O−H···N, N−H···O, and N−H···N) involving the amino and hydroxyl protons of carboxylic acid as donors and the two pyrimidine nitrogens including the oxygen of the carboxyl group as acceptors. Adjacent tetramers are connected via C−H···O hydrogen bond, involving the C−H and the oxygen of methoxy group of pyrimidine ring on either side (C8−H8C···O8). As a result adjacent tetramers are assembled into infinite 1-D tapes (Figure 3). However this time, in contrast to the previous structure, each tape is not interconnected with the neighboring ones through C−H···O bonds since they lie far away from each other. They also form a

Table 2. Hydrogen Bond Metrics for Compounds 1−14

D- - -H⋯A	H⋯A (Å)	D⋯A (Å)	∠D—H⋯A	symmetry operation
		MOP·2CBA (1:1)		
O(1)- - -H(1)⋯N(1)	1.89	2.699(2)	171	*x, y, z*
N(2)- - -H(2A)⋯N(3)	2.31	3.156(2)	166	*2 − x, −y, 1 − z*
N(2)- - -H(2B)⋯O(2)	1.97	2.829(2)	173	*x, y, z*
C(8)- - -H(8B)⋯O(8)	2.59	3.473(2)	152	*−x, 1 − y, 1 − z*
C(12)- - -H(12)⋯O(7)	2.52	3.415(2)	161	*x, 1 + y, −1 + z*
		MOP·3MBA (1:1)		
O(1)- - -H(1)⋯N(1)	1.87	2.6817(19)	168	*x, y, z*
N(2)- - -H(2A)⋯N(3)	2.31	3.161(2)	169	*2 − x, −y, 1 − z*
N(2)- - -H(2B)⋯O(2)	2.06	2.912(2)	173	*x, y, z*
C(8)- - -H(8C)⋯O(8)	2.58	3.458(2)	151	*−x, 1 − y, 1 − z*
		MOP·CA (1:1)		
O(1)- - -H(1)⋯N(1)	1.90	2.712(2)	169	*x, y, z*
N(2)- - -H(2A)⋯O(2)	2.02	2.878(2)	174	*x, y, z*
N(2)- - -H(2B)⋯N(3)	2.28	3.130(2)	169	*−x, −y, −z*
C(14)- - -H(14)⋯O(1)	2.68	3.565(2)	159	*2 − x, 1 − y, 1 − z*
		MOP·4NBA (1:1)		
O(1)- - -H(1)⋯N(1)	1.83	2.643(2)	170	*x, y, z*
N(2)- - -H(2A)⋯O(2)	2.01	2.869(2)	173	*x, y, z*
N(2)- - -H(2B)⋯N(3)	2.29	3.098(2)	157	*2 − x,1 − y, 1 − z*
		MOP·4MOBA (1:1)		
O(1)- - -H(1)⋯N(1)	1.91	2.7270(15)	172	*x, y, z*
N(2)- - -H(2A)⋯O(2)	2.11	2.9142(17)	155	*1 − x, 1 − y, 1 − z*
N(2)- - -H(2B)⋯O(2)	2.00	2.8479(18)	170	*x, y, z*
		MOP·IPA (2:1)		
O(1)- - -H(1)⋯N(1A)	1.97	2.7807(16)	172	*x, y, z*
N(2A)- - -H(2A1)⋯O(2)	1.99	2.8267(19)	166	*x, y, z*
O(3)- - -H(3A)⋯N(1B)	1.85	2.6606(18)	170	*x, y, z*
N(2B)- - -H(2B1)⋯O(4)	2.00	2.851(2)	168	*x, y, z*
N(2B)- - -H(2B2)⋯O(7A)	2.21	2.976(2)	149	*2 − x,1 − y, −z*
C(7B)- - -H(7B3)⋯O(2)	2.55	3.433(2)	153	*x, 1 + y, 1 + z*
		MOP·CAA (1:1)		
O(1)- - -H(1)⋯N(1)	1.82	2.6351(18)	170	*x, y, z*
N(2)- - -H(2A)⋯O(2)	1.99	2.8495(18)	173	*x, y, z*
N(2)- - -H(2B)⋯N(3)	2.34	3.187(2)	167	*1 − x, 2 − y, 1 − z*
		MOP⁺·TCAA⁻ (1:1)		
N(1)- - -H(1)⋯O(1)	1.89	2.734(2)	165	*x, y, z*
N(2)- - -H(2A)⋯O(2)	2.16	2.845(2)	137	*1 − x, 1 − y, 1 − z*
N(2)- - -H(2B)⋯O(2)	1.93	2.786(2)	175	*x, y, z*
		MO⁺P·5CSA⁻ (1:1)		
N(1)- - -H(1)⋯O(1)	1.80	2.6582(15)	178	*x, y, z*
N(2)- - -H(2A)⋯N(3)	2.32	3.1627(18)	166	*x, 3/2 − y, 1/2 + z*
N(2)- - -H(2B)⋯O(2)	1.94	2.7742(18)	165	*x, y, z*
O(3)- - -H(3)⋯O(2)	1.81	2.5273(18)	145	*x, y, z*
C(7)- - -H(7B)⋯O(1)	2.42	3.3311(18)	160	*1 − x, 1 − y, 1 − z*
		MOP⁺·3HPA⁻ (1:1)		
N(2A)- - -H(2A1)⋯N(4A)	2.10	2.9571(17)	172	*1 − x, 1 − y, −z*
N(1A)- - -H(1A)⋯O(1A)	1.86	2.7146(14)	176	*x, y, z*
N(2A)- - -H(2A2)⋯O(2A)	1.94	2.7870(16)	168	*x, y, z*
O(3A)- - -H(3A)⋯O(1A)	1.80	2.5280(17)	147	*x, y, z*
N(1B)- - -H(1B)⋯O(1B)	1.83	2.6934(14)	178	*x, y, z*
O(3B)- - -H(3B)⋯O(1B)	1.79	2.5214(17)	148	*x, y, z*
N(2B)- - -H(2B1)⋯N(4B)	2.20	3.0491(19)	172	*2 − x, 1 − y, 1 − z*
N(2B)- - -H(2B2)⋯O(2B)	1.94	2.7885(16)	169	*x, y, z*
C(8B)- - -H(8B3)⋯O(8B)	2.66	3.5781(15)	161	*1 − x, −y, 1 − z*
		MP⁺·5CSA⁻ (1:1)		
N(2A)- - -H(2A1)⋯O(2B)	1.99	2.799(6)	158	*x, y, z*
N(2B)- - -H(2B1)⋯O(2A)	2.02	2.833(5)	156	*x, y, z*
N(2A)- - -H(2A2)⋯O(2A)	1.95	2.790(6)	167	*x, y, z*
N(2B)- - -H(2B2)⋯O(2B)	1.93	2.792(5)	176	*x, y, z*
N(1A)- - -H(1A)⋯O(1A)	1.82	2.678(6)	175	*x, y, z*

Table 2. continued

D- - -H···A	H···A (Å)	D···A (Å)	∠D—H···A	symmetry operation
		MP⁺·5CSA⁻ (1:1)		
N(1B)- - -H(1B···O(1B)	1.87	2.728(5)	175	*x, y, z*
O(3A)- - -H(3A)···O(1A)	1.80	2.524(5)	147	*x, y, z*
O(3B)- - -H(3B)···O(1B)	1.79	2.523(5)	147	*x, y, z*
C(5A)- - -H(5A)···O(3B)	2.53	3.375(6)	151	*1 − x, 1/2 + y, 3/2 − z*
C(5B)- - -H(5B)···O(3A)	2.56	3.401(6)	150	*−x, −1/2 + y, 1/2 − z*
		MP⁺·MA⁻ (1:1)		
N(1)- - -H(1)···O(1)	1.79	2.652(2)	175	*x, y, z*
N(2)- - -H(2A)···N(3)	2.14	2.998(2)	179	*1 − x, 1 − y, −z*
N(2)- - -H(2B)···O(2)	1.92	2.775(2)	170	*x, y, z*
O(3)- - -H(3)···O(2)	1.72	2.482(2)	155	*x, y, z*
C(5)- - -H(5)···O(3)	2.61	3.401(3)	139	*2 + x, −1 + y, z*
		MP·GA (2:1)		
O(1)- - -H(1)···N(1A)	1.82	2.612(7)	161	*x, y, z*
N(2A)- - -H(2A1)···N(3B)	2.19	3.047(7)	172	*1/2 + x, −y, z*
N(2A)- - -H(2A2)···O(2)	2.10	2.948(8)	169	*x, y, z*
O(3)- - -H(3)···N(1B)	1.82	2.606(7)	160	*x, y, z*
N(2B)- - -H(2B1)···O(4)	2.11	2.960(8)	168	*x, y, z*
N(2B)- - -H(2B2)···N(3A)	2.21	3.053(8)	168	*−1/2 + x, −y, z*
		MP·AA (2:1)		
O(1)- - -H(1)···N(1A)	1.85	2.649(3)	165	*x, y, z*
N(2A)- - -H(2A1)···O(2)	2.14	2.993(3)	170	*x, y, z*
N(2A)- - -H(2A2)···N(3B)	2.19	3.045(3)	171	*1 + x, y, −1 + z*
O(3)- - -H(3)···N(1B)	1.86	2.659(3)	165	*x, y, z*
N(2B)- - -H(2B1)···N(3A)	2.18	3.043(3)	177	*−1 + x, y, 1 + z*
N(2B)- - -H(2B2)···O(4)	2.13	2.980(3)	173	*x, y, z*
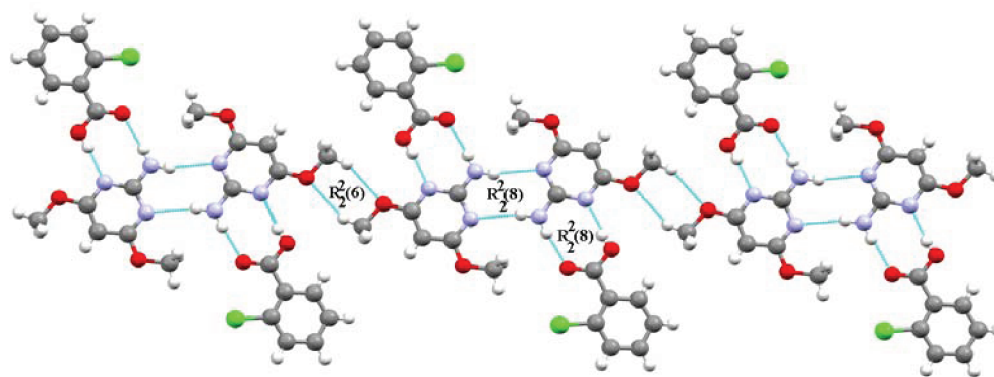
Figure 1. View of infinite tape connected by $R_2^2(6)$ synthon in **1**.

planar sheet (Figure 4) along the (122) plane which stacks one over the other through Π−Π interactions. The stacking interactions are similar to the previous structure which occur between two pyrimidine and two acid moieties with Cg−Cg distance of 3.4113(9) and 3.9030(12) Å and a slip angle of 7.98° and 15.36°, respectively.

2-Amino-4,6-dimethoxypyrimidine-cinnamic Acid (3). **3** also crystallizes in triclinic $P\overline{1}$ space group. The asymmetric unit consists of a molecule of CA and MOP. A similar four component supermolecule (linear heterotetramer) is formed which is essentially the same like the previous structures. The adjacent tetrameric units are held together through inversely related C14−H14···O1 hydrogen bonds, involving C−H of the acid ring and hydroxyl oxygen of carboxylic group in the acid molecule, to form an infinite 1D tape (Figure 5). These parallel tapes lie alongside each other in the $(11\overline{3})$ plane (Figure 6).

Stacking interactions between these parallel sheets of molecules are far from the expected range.

2-Amino-4,6-dimethoxypyrimidine-4-nitrobenzoic Acid (4). MOP.4NBA crystallizes in monoclinic $P2_1/c$ space group with a molecule of MOP and 4NBA in the asymmetric unit. The primary supermolecule in the crystal structure are connected through the acid and amino-pyrimidine moieties engaging in O−H···N and N−H···O hydrogen bonds. The secondary synthons involving the N−H···N hydrogen bonds are responsible for the formation of the linear heterotetramer. All the heterotetramers do not lie in the same plane unlike the previous structures rather they are in two different planes. Inspite of the presence of the two strong acceptor atoms (oxygen atoms of the nitro group in the aromatic acid), no extra hydrogen bonds are found within the limits. Moreover no stacking interactions are observed in this structure.
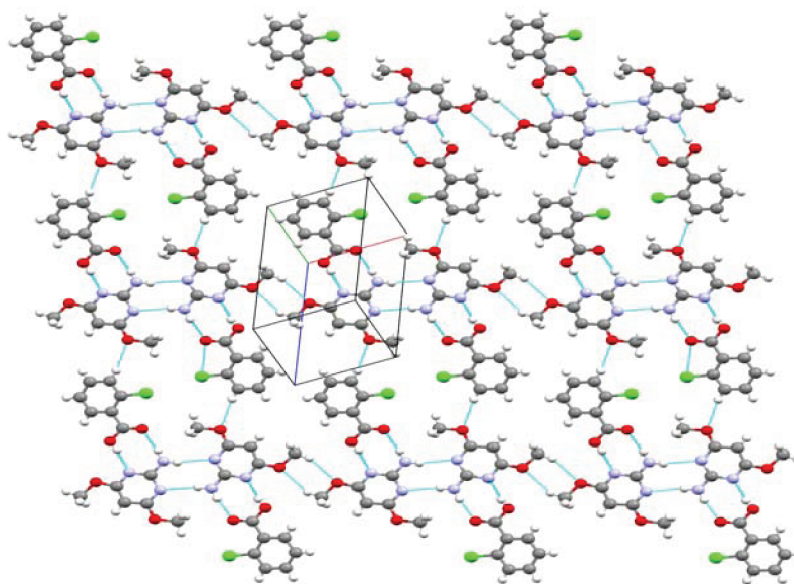
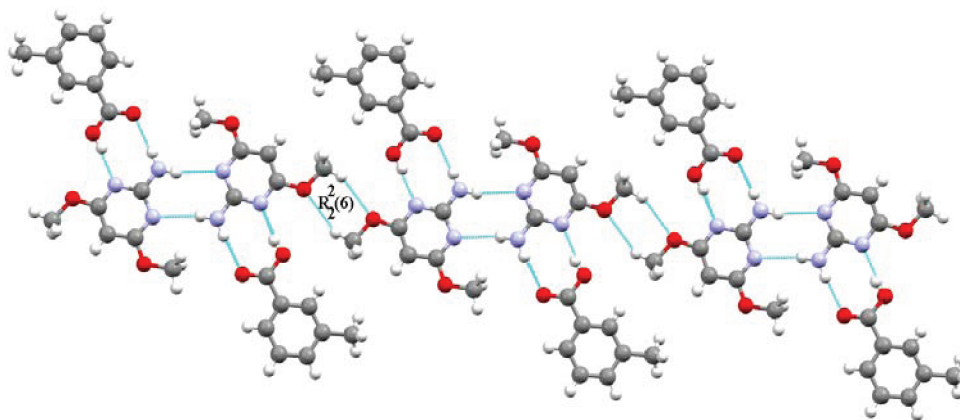**Figure 2.** Supramolecular sheet formed by interconnection of tapes along (122) plane in **1**.

Figure 3. Extension of infinite tape connected by $R_2^2(6)$ synthon in **2**.

2-Amino-4,6-dimethoxypyrimidine-4-methoxyben-zoic Acid (5). MOP·4MOBA crystallizes in the $P2_1/c$ monoclinic space group where the asymmetric unit consists of single molecule of 4MOBA acid and MOP. A couple of N−H···O and O−H···N hydrogen bonds is responsible for the formation of a dimer which acts as the primary hydrogen bonds. The two acid-aminopyrimidine dimers are again interlinked together with N−H···O bonds (secondary hydrogen bonds) between the free amino H-atom of one of the dimer and the carbonyl oxygen of the acid in the other dimer producing a DADA (D-hydrogen bonded donor and A- hydrogen bonded acceptor) array of quadruple hydrogen bonds which is represented by graph-set notation $R_2^2(8)$, $R_4^2(8)$, and $R_2^2(8)$ to form a cyclic heterotetrameric synthon (Figure 7). These tetramers are also arranged in a two-dimensional pattern without any neighboring interaction along the ($21\bar{1}$) plane. There are two types of Π−Π stacking noted between the aminopyrimidine and the acid moieties. The pyrimidine ring present in a plane, exhibits stacking interactions with both acid molecules lying in parallel planes above and below it with Cg−Cg distance of 3.6309(8) and 3.8526(8) Å and a slip angle of 15.38° and 25.35°, respectively (Figure 8).

2-Amino-4,6-dimethoxypyrimidine-isophthalic Acid (6). **6** crystallizes in triclinic $P\bar{1}$ space group with two crystallographically independent molecules of MOP and one molecule of IPA in the asymmetric unit. The trimer in the crystal is the result of hydrogen-bond interactions between the two carboxylic acid groups in IPA and the two MOP molecules. The primary synthons in this structure are N−H···O and O−H···N hydrogen bonds. In the 2:1 ligand-acid trimer, the free amino proton in the B molecule of the pyrimidine moiety interacts with an oxygen of the methoxy group in the neighboring trimer (symmetry code $2 − x$, $1 − y$, $−z$) to form a hexameric supermolecule via N2B−H2B2···O7A hydrogen bonds (Figure 9). One of the amino group hydrogens (H2A of the A pyrimidine molecule) and pyrimidine nitrogens (N3 of both pyrimidine molecules) in pyrimidine moiety have not participated in any of the hydrogen bonding interactions. The reason could be the presence of two methoxy groups lying adjacent to each other in the hexameric supermolecule which sterically hinders any donor hydrogens from approaching the acceptors. The oval-shaped hexameric supermolecules are further fused to neighboring ones through weak C−H···O bonds (symmetry code x, $1 + y$, $1 + z$) and extends itself along a direction to form a tape. Many parallel tapes lie alongside on the ($1\bar{2}2$) plane as shown in Figure 10.
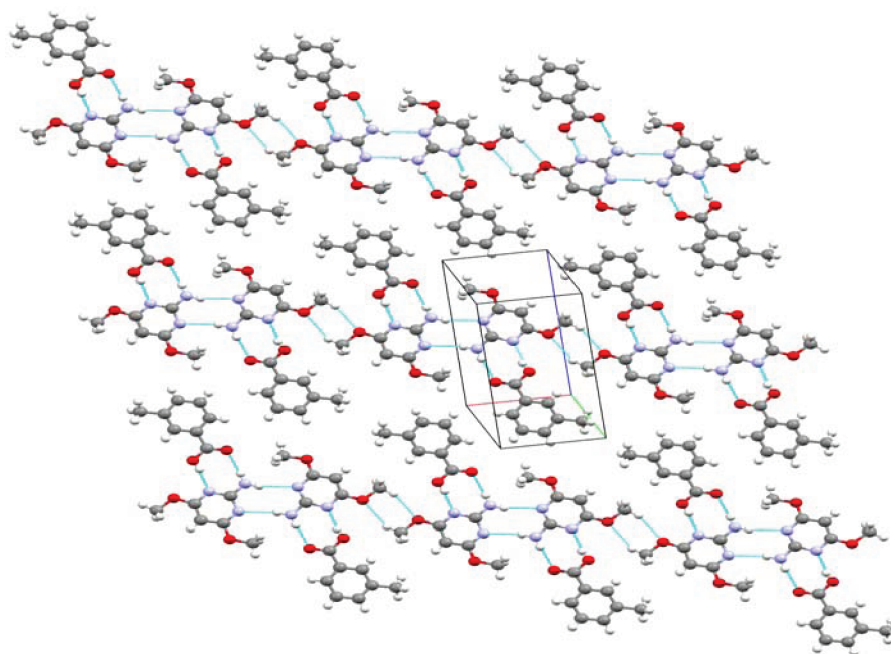
Figure 4. Supramolecular sheet along (122) plane with no interaction by neighboring tapes in **2**.
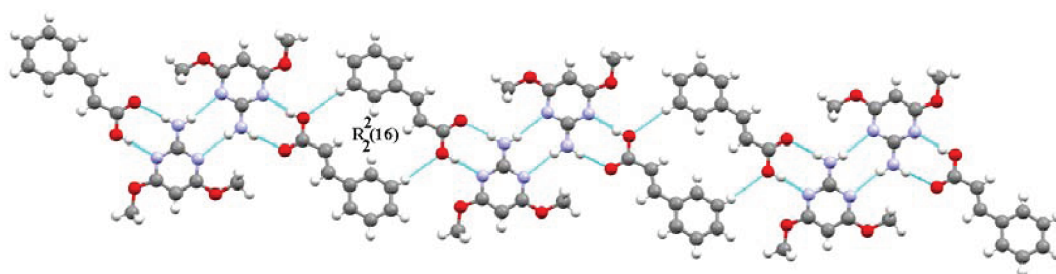

Figure 5. Extension of infinite tape connected by $R_2^2(16)$ synthon in **3**.

Two types of Π−Π stacking are noted; one between the pyrimidine−acid and the other between two pyrimidine−pyrimidine moieties. The tapes that extend along a one-dimensional direction stack with adjacent tapes, one lying on top (through pyrimidine A−acid stacking) and the other at the bottom (pyrimidine A−pyrimidine B stacking) with Cg−Cg distance of 3.6971(9) and 3.7526(8) Å and a slip angle of 21.23° and 23.47°, respectively.

2-Amino-4,6-dimethoxypyrimidine-chloroacetic Acid (7) and 2-Amino-4,6-dimethoxypyrimidinium Trichloroacetate (8). Both **7** and **8** crystallizes in the same monoclinic $P2_1/c$ space group. The asymmetric unit of **7** contains a neutral molecule of MOP and CAA like the previous cases whereas **8** consists of a pyrimidinium cation (MOP⁺) and a triacetate anion (TCAA⁻). The pyrimidinium cation is a consequence of the proton transfer from the acid to the pyrimidine ring. This is reflected by an increase in C−N−C bond angle compared to the neutral molecule.

The primary motif in **7** is composed of MOP and CAA which is connected through a couple strong hydrogen bonds (O−H···N and N−H···O hydrogen bonds), whereas in **8**, it is made up of charge-assisted hydrogen bond interactions between the carboxylate and the amino-pyrimidinium moieties through N−H···O⁻ and N−H⁺···O⁻ hydrogen bonds. In **7**, the secondary N−H···N hydrogen bonds formed from the amino proton and

the N3 pyrimidine nitrogen atom extends the architecture into a four-component supermolecule which is a linear heterotetramer. These supermolecules align themselves along a line without any strong interaction to form a chain (although a formation of $R_2^2(6)$ motif is viable, the hydrogen bonds are not within range). Such type of chains interpenetrate between each other in almost perpendicular direction and look like a three-dimensional grid (Figure 11). No stacking interactions are observed in this structure.

Similarly secondary N−H···O⁻ hydrogen bonds, formed from the free amino proton and the carbonyl oxygen, extend **8** into a four-component cyclic heterotetramer with DDAA array of quadruple hydrogen bonds. The cyclic tetramer extends itself by interacting through Cl···O bonds (involving Cl2 of the trichloroacetate anion and O1 of the heterocycle), with Cl2···O1 distance of 3.2192(16) Å and C−Cl···O angle of 162.2° (18) along the x-axis to form a supramolecular tape (Figure 12). The supramolecular tapes are interconnected to the neighboring ones through chlorine-chlorine interaction with Cl···Cl distance of 3.4675(9) Å. No stacking interactions are present in this structure (Figure 13).

2-Amino-4,6-dimethoxypyrimidinium 5-chlorosalicylate (9). The crystal structure of **9** crystallizes in orthorhombic *Pbca* space group. The asymmetric unit contains one MOP⁺ cation and one 5CSA⁻ anion. After the formation of a dimer
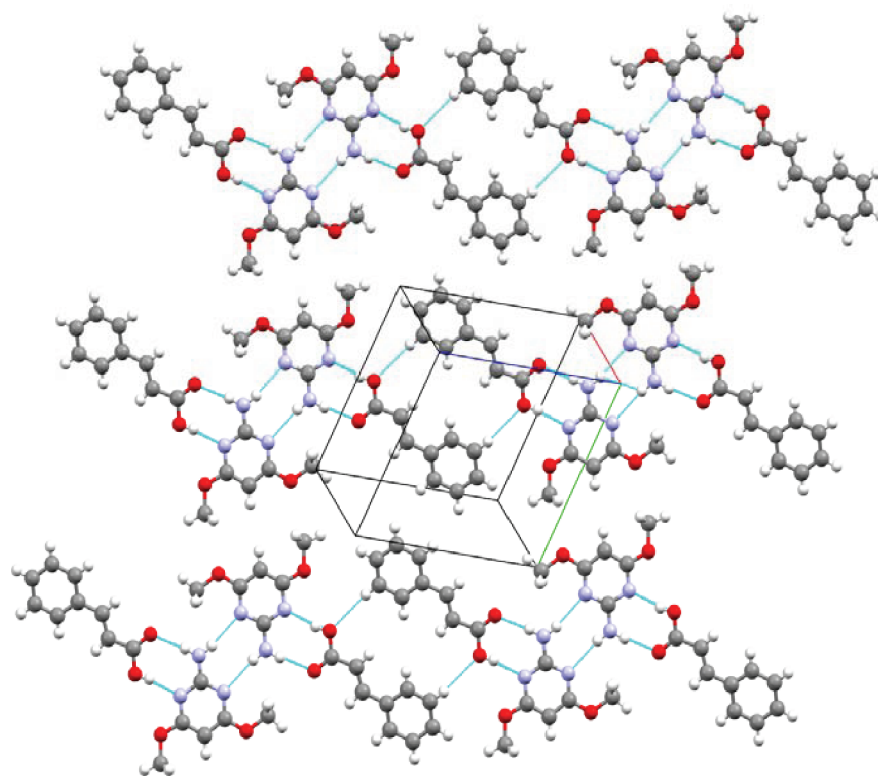
Figure 6. Supramolecular sheet along (11$\bar{3}$) plane without interaction by adjacent tapes in **3**.
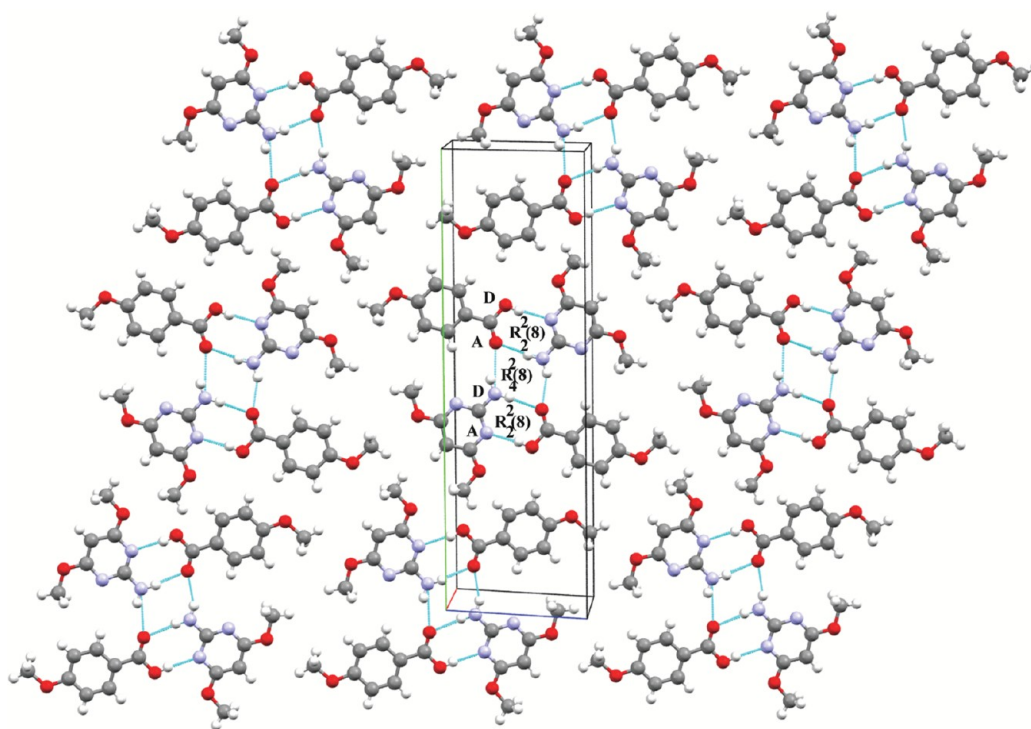

Figure 7. Supramolecular sheet formed by cyclic tetramers in **5** along (21$\bar{1}$) plane with no interaction by neighboring ones.

through the primary synthons (charge-assisted N−H···O$^-$ and N−H$^+$···O$^-$ hydrogen bonds between the carboxylate and the amino-pyrimidinium moieties) in the crystal structure of **9**, the secondary N−H···N hydrogen bonds take over to form the four-component linear heterotetramer. In the anion, a typical intramolecular hydrogen bond is formed between the hydroxyl

group and the carboxylate anion with graph-set notation S(6). Weak C−H···O bonds, involving the C−H of the methoxy group and the carbonyl oxygen of the anion (C7−H7B···O1 hydrogen bond), link the dimers to form a zigzag supramolecular chain along the *c*-axis (Figure 14). Adjacently arranged tetramer units in two different planes are stacked through Π−Π interactions
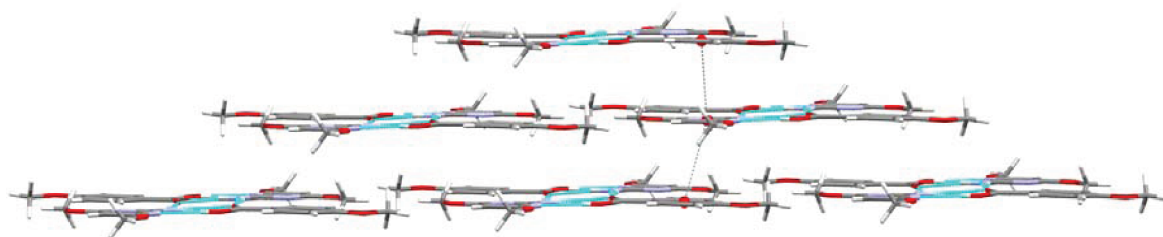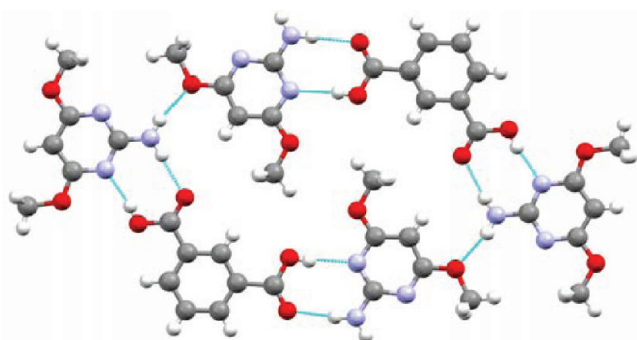
Figure 8. Stacking between two different planes in **5**.

Figure 9. View of hexameric supermolecule in **6**.

Figure 11. View of a segment of interpenetrated chains that form grid like structure in **7**.

between an anion and a pyrimidinium base with Cg–Cg distance of 3.6916(9) Å and a slip angle of 19.94° (Figure 15).

2-Amino-4,6-dimethoxypyrimidinium 3-hydroxypico-linate (10). MOP$^+$·3HPA$^-$ crystallizes in triclinic space group $P\bar{1}$ with the asymmetric unit containing two MOP$^+$ cations and two 3HPA$^-$ anions. The formation of an organic salt is confirmed from the protonation at the pyrimidine ring (evident from the increase in C–N–C bond angle compared to the neutral molecule). The salt displays exactly the same primary motif exhibited by MOP$^+$·TCAA$^-$ and MOP$^+$·5CSA$^-$, composed of intermolecular interactions: N–H...O$^-$ and N–H$^+$...O$^-$. The primary motif is interlinked by the free amino hydrogen atom and the acceptor nitrogen in the picolinate anion through secondary hydrogen bonds to form a cyclic heterotetramer
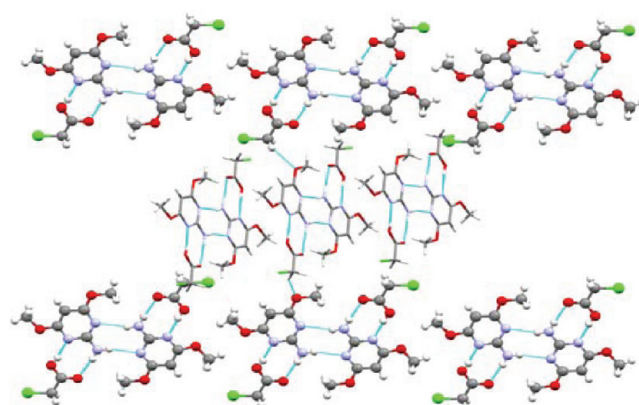
distinct from the other two cases. Typical intramolecular hydrogen bond exists between the hydroxyl –OH group and the carboxylate group of the 3-hydroxypicolinate anion to form a six-membered hydrogen-bonded ring [S(6)]. The two molecules in the asymmetric unit initially form the same type of cyclic heterotetramer and differ only in the further aggregation. The cyclic heterotetramers formed by both molecules (A and B) arrange themselves along a plane in different ways to form a long strip of tape propagating along different directions (Figure 16). Molecule A does not involve in any hydrogen bonds to form the tape whereas molecule B links the neighboring ones through
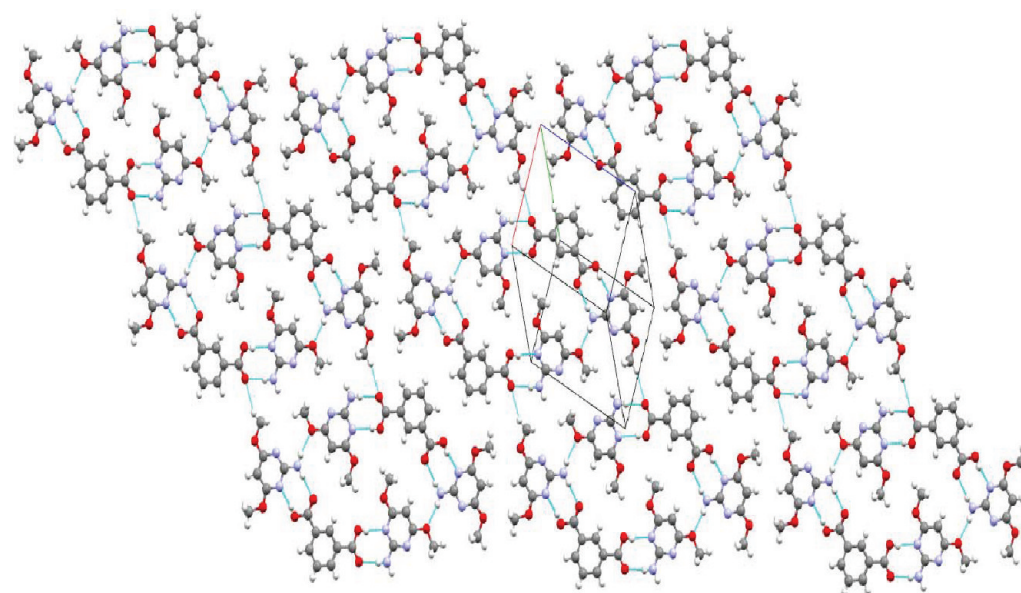

Figure 10. Supramolecular sheet in **6** formed by hexamers along $(1\bar{2}2)$ plane with no interaction by neighboring tapes.
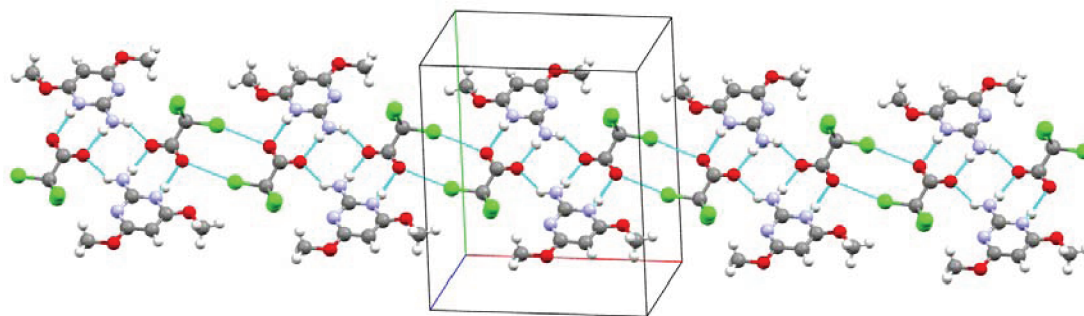
Figure 12. View of supramolecular tape formed through chlorine−oxygen interaction in **8**.
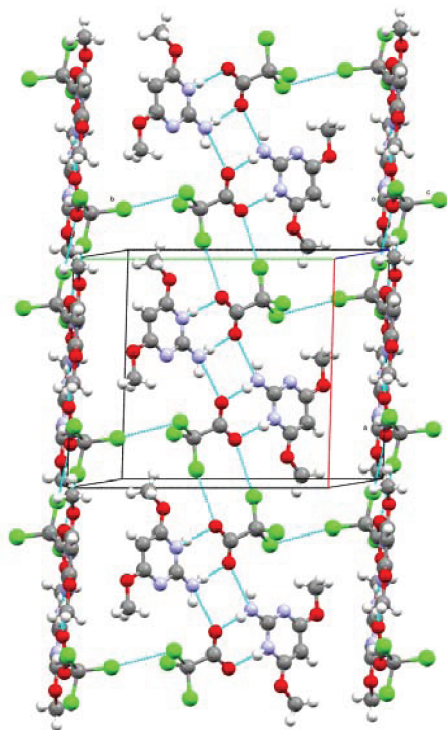

Figure 13. Interlinking of adjacent tapes through Cl···Cl interation in **8**.

weak C8B−H8B3···O8B bonds involving the $R_2^2(6)$ motif (symmetry code $1 − x, −y, 1 − z$). Both tapes lie crisscross in the overall pattern to form a grid like network as shown in Figure 17.

2-Amino-4,6-dimethylpyrimidinium 5-chlorosalicylate (11). The crystal structure **11** crystallizes in monoclinic $P2_1/c$ space group. The asymmetric unit contains two crystallographically independent MP$^+$ cations and 5CSA$^-$ anions.

MP$^+$·5CSA$^-$ is also a salt which is confirmed by the protonation at the N1 position, reflected by an increase in C−N−C bond angle compared to the neutral molecule. The two independent molecules look almost identical with one another having similar molecular interactions. They differ from each other with slight variations in the bond distances, bond angles and hydrogen bond lengths. The two crystallographically independent molecules are related by pseudosymmetry. All alternate space groups are eliminated by an analysis using PLATON. The primary synthons are formed as result of two sets of inequivalent charge-assisted N−H···O$^-$ and N−H$^+$···O$^-$ hydrogen bonds in structure **11**. The ion pairs are linked through charge-assisted N−H···O$^-$ formed from the free amino proton and carboxylate moiety to form a cyclic heterotetramer. The tetramer is composed of small motifs (represented by the graph-set notation $R_2^2(8)$, $R_4^2(8)$, and $R_2^2(8)$) leading to DDAA array of quadruple hydrogen bonds as in the case of **8**. These larger synthons in turn aggregate in (−101) plane through C5A−H5A···O3B and C5B−H5B···O3A hydrogen bonds involving a larger ring motif to form a supramolecular sheet as shown in Figure 18.

2-Amino-4,6-dimethylpyrimidinium hydrogen malonate (12), 2-Amino-4,6-dimethylpyrimidine-glutaric acid (13), and 2-Amino-4,6-dimethylpyrimidine-adipic Acid (14). **12** crystallizes in triclinic $P\bar{1}$, **13** in orthorhombic $Pca2_1$ and **14** in $P2_1/c$ space groups. MP·GA and MP·AA are sustained by three-molecule aggregates consisting of two molecules of MP and one molecule of acid in the asymmetric unit whereas MP$^+$·MA$^-$ consists of a single MP$^+$ cation and a single MA$^-$ anion in the asymmetric unit. The primary synthons in **12** are charge-assisted N−H$^+$···O$^-$ and N−H···O$^-$ hydrogen bonds forming a dimer. The dimer is linked to one end by a cation through base pair (couple of N−H···N bonds) and the other end by an anion through a pair of weak C−H···O bonds involving the C−H of methylene carbon and the carboxylate oxygen extending itself into a zigzag tape with three different $R_2^2(8)$ motifs. These zizzag
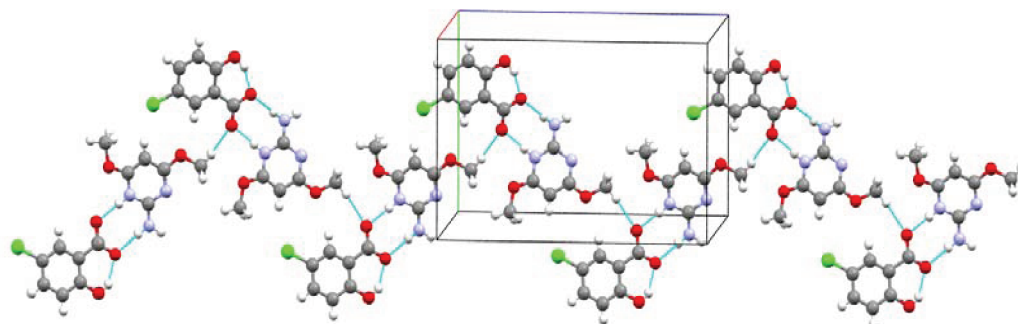

Figure 14. Formation of supramolecular chain through weak C−H···O interaction in **9**.
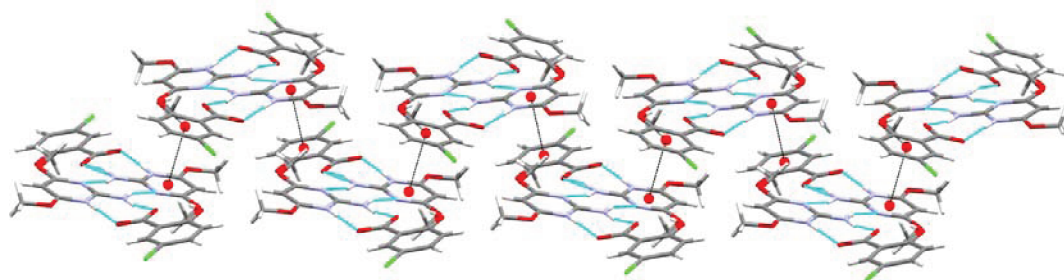
Figure 15. Stacking interactions observed between two aminopyrimidine rings in **9** is shown.
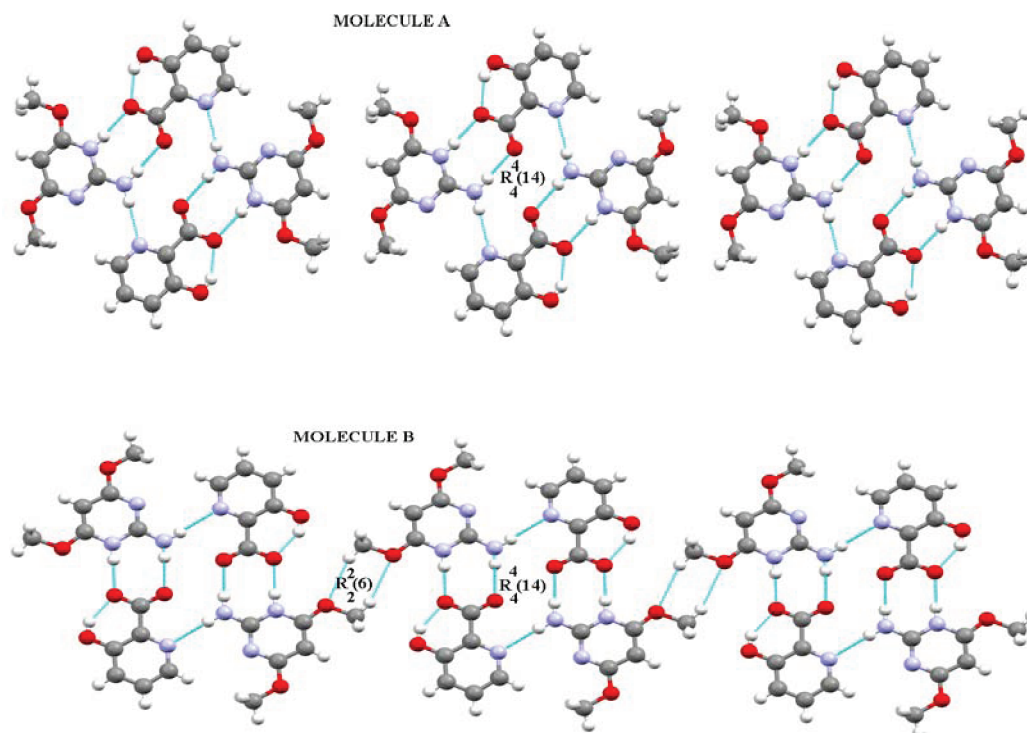

Figure 16. Tetramers of molecule A lying alongside each other and of molecule B connected via $R_2^2(6)$ synthon to form a supramolecular tape in **10**.
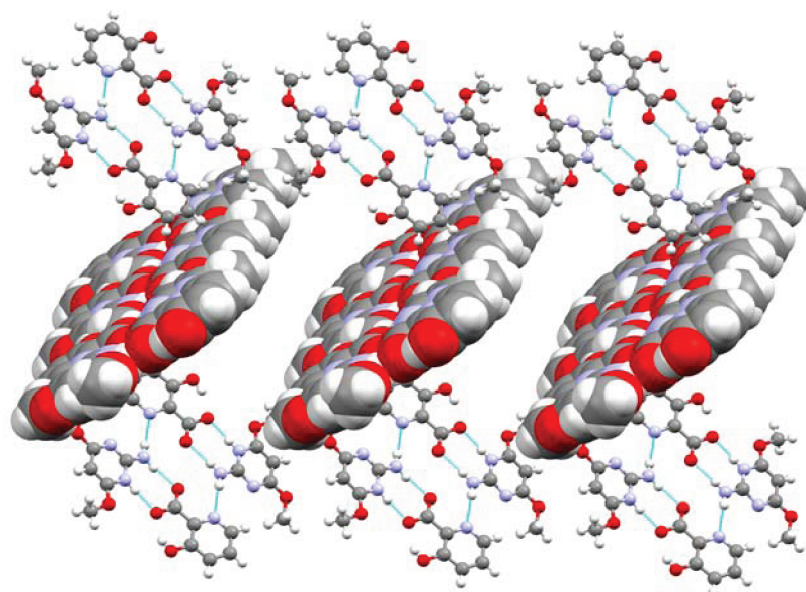

Figure 17. View of interpenetrated strips of molecule A (represented by ball and stick) and molecule B (represented by space filled mode) in **10**.
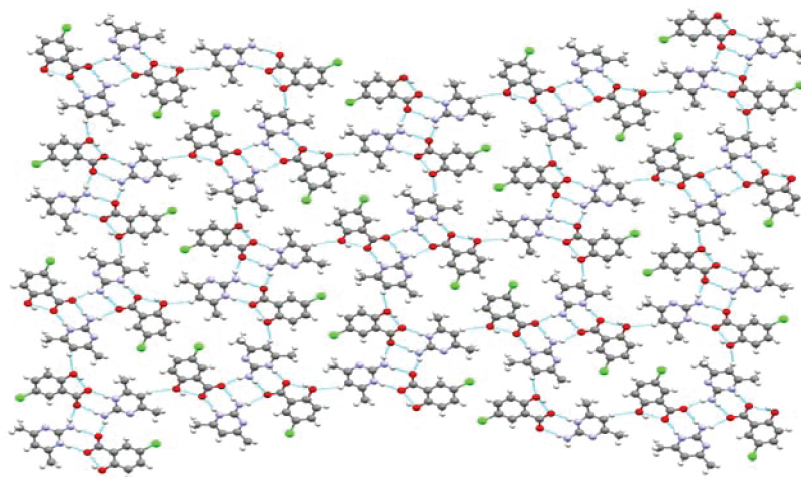
Figure 18. Interlinking cyclic heterotetramers through weak C−H···O bonds leads to the formation of supramolecular sheet in **11**.
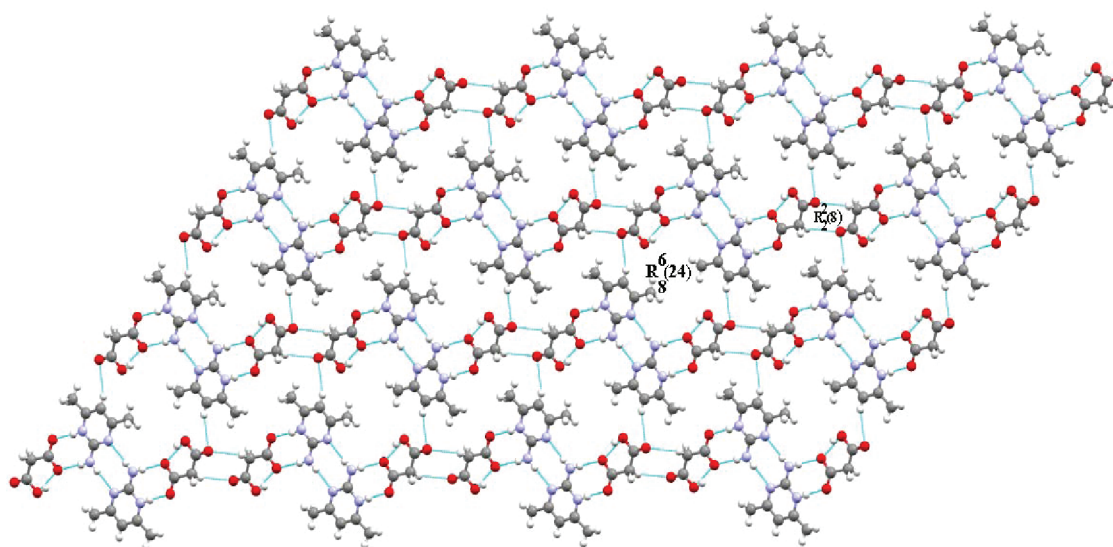

Figure 19. View of supramolecular corrugated sheet along (120) plane in **12**.

tapes are interlinked through C5−H5···O5 bonds with neighboring ones to form a planar corrugated sheet along the (120) plane (Figure 19). In **13** and **14**, the primary intermolecular O−H···N and N−H···O hydrogen bonds between dicarboxylic acids and MP are essentially the same on both sides of the diacid. The trimers are again arranged into extended 1-D zigzag infinite chains connected by the terminal MP at both ends through base pairing (Figure 20 and 21). In both the compounds, alternative chains have a similar pattern of arrangements having their base pair aligned in a same direction whereas the neighboring symmetry related chains have the base pair aligned in the opposite direction. The difference lies only in the dimensionality maintained by both the structures. The zigzag chains arranged in **14** lie along the same plane unlike **13** showing 3D nature. The planes of the two carboxylic acid moieties (involving the carbonyl carbon and the two oxygen atoms) in **14** are slightly twisted with respect to each other, having an angle of 4.82°, which suggests that the trimeric supermolecule is almost in a single plane which in turn leads to a planar arrangement of the entire zigzag chains along the (101) plane. In **13**, the angle of twist between both carboxylic acid groups with respect one another is 79.38°, which eventually

leads to the nonplanar trimer. The extended infinite chain obviously lies out of plane unlike **14**. No stacking interactions are found in both **12** and **13**. The planar sheets of **14** are stabilized through Π−Π stacking interactions between two of the pyrimidine B molecules with interplanar distance, Cg−Cg distance and slip angle of 3.4698(9) Å, 3.6048(13) Å and 15.73° respectively (Figure 22).

■ DISCUSSION

By using Cambridge Structural Database (CSD), several recurrently occurring hydrogen-bonded synthons have been recognized and identified by Desiraju and Allen et al.[22,23,51] One such frequently occurring bimolecular cyclic hydrogen bonded synthon is a ring motif with graph set notation, $R_2^2(8)$, which is readily formed between a carboxylic acid and an aminopyrimidine group. However we are much interested on what happens after this step and how they go on to self-assemble into larger supramolecular assemblies.

In the present study, several small and large sized ring motifs are observed, such as $R_2^2(6)$, $R_2^2(8)$, $R_4^2(8)$, $R_4^4(14)$, $R_2^2(16)$, $R_6^4(22)$, $R_8^6(24)$, and $R_6^6(32)$. But not all of them occur
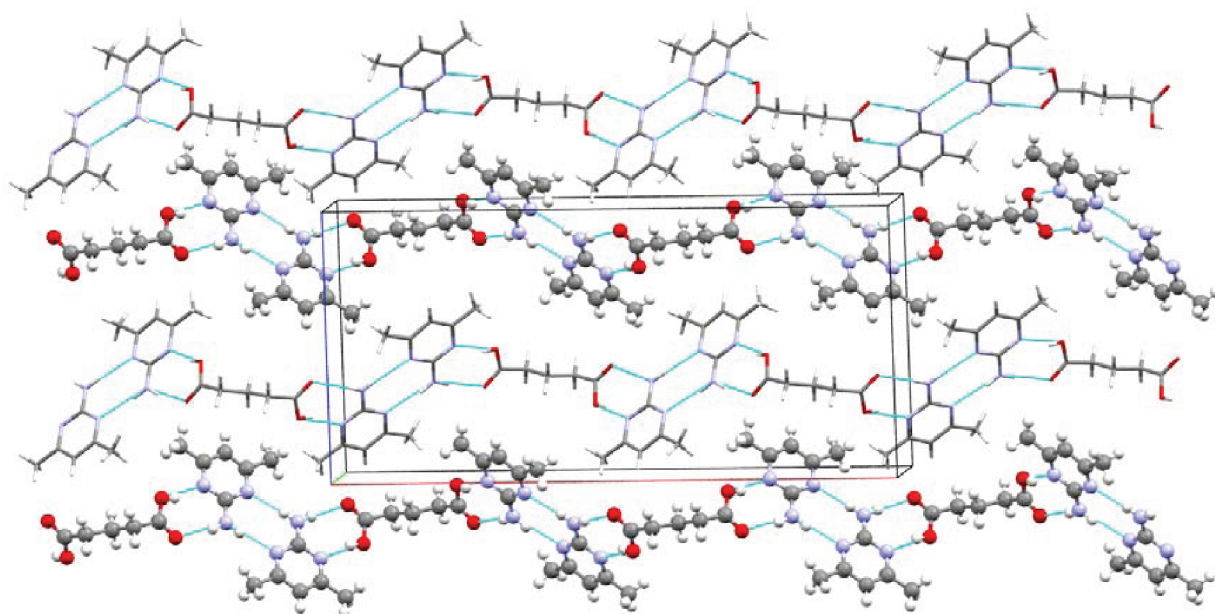
Figure 20. Infinite zigzag chains formed in **13**.
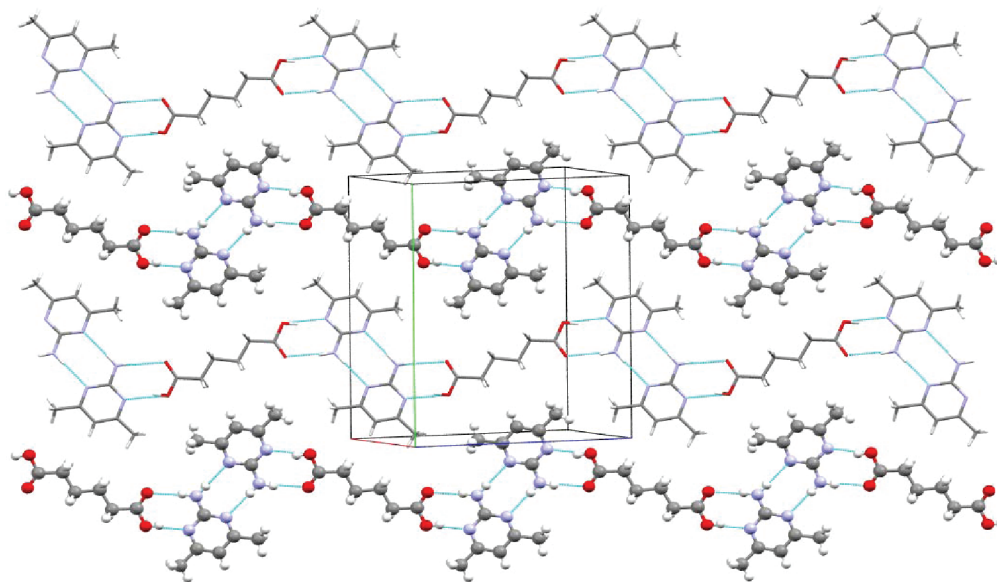

Figure 21. Infinite zigzag chains of **14** lying parallel to each other along the (101) plane.
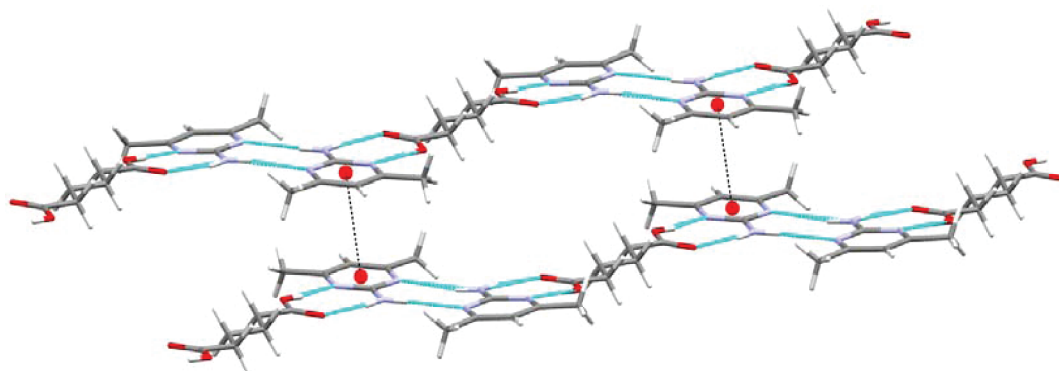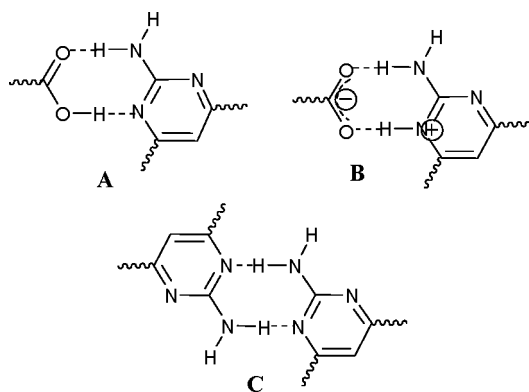

Figure 22. Π−Π stacking between pyrimidines moieties of different planar chains in **14**.

3779

dx.doi.org/10.1021/cg3005954 | *Cryst. Growth Des.* 2012, 12, 3766−3785

Scheme 2. Three Types of $R_2^2(8)$ Motifs

repeatedly, as most of them arise only in specific cases. Nevertheless $R_2^2(6)$, $R_2^2(8)$, and $R_4^2(8)$ motifs have been the most recurrently occurring ones in the present study. Among the three the later two are involved through the formation of strong hydrogen bonds whereas the former one is formed through weak bonds. The high-probability $R_2^2(8)$ motif is special because they emerge through three different ways (by involvement of different hydrogen bonds) as shown in Scheme 2.

In all the 14 structures, the primary motif is the formation of pyrimidine-carboxylic acid dimer through the predominant $R_2^2(8)$ synthon. The primary intermolecular bonds involved are the O−H···N/O⁻···H−N⁺ and N−H···O/N−H···O⁻ bonds and it is only in next step that the higher levels of structural

changes are observed. Subsequent levels of aggregation form either a linear heterotetramer (LHT) or cyclic heterotetramer (CHT) or heterotrimer (HT) or any other preferred stable synthon. Scheme 3 shows the common synthons that are formed while Table 3 and Table 4 lists out the type of synthons involved in each of the molecular complexes.

Among the 14 structures, 9 of them readily form linear hetero-tetrameric synthon (**1**, **2**, **3**, **4**, **7**, **9**, **12**, **13**, and **14**), 3 of them form a cyclic tetramer (**5**, **8**, and **11**), 1 of them forms a trimer (**6**), and the other (**10**) forms a relatively different type of cyclic tetramer.

The 9 linear heterotetramers are formed by the combination of three $R_2^2(8)$ motifs. Structures **1**, **2** and **3** have the linear tetramers arranged in a plane and incidentally all of them have crystallized in the same space group, P-1. Each linear tetramer is surrounded by six such tetramers in proximity to form a planar sheet as shown in Figure 23. The similar type of arrangement of the sheets has lead the closeness in the lattice parameters in structure **1** and **2** but not **3**. This is explained by the fact that the linear heterotetramers in **1** and **2** are connected to its neighbor through $R_2^2(6)$ motif whereas **3** has not got the luxury because of its structural chemistry. Tetrameric structures **4**, **7**, and **9** do not lie in a plane and therefore have distinct patterns. **12** also forms a linear heterotetramer like the rest of the structures and further organizes through other hydrogen bonds to form larger supramolecular architectures. Although **13** and **14** give the impression that they have formed a heterotrimer initially, the extended trimeric infinite chain has revealed that they are built

Scheme 3. Representation of Three Types of Synthons Formed by Combination of Pyrimidine and Carboxylic Acid
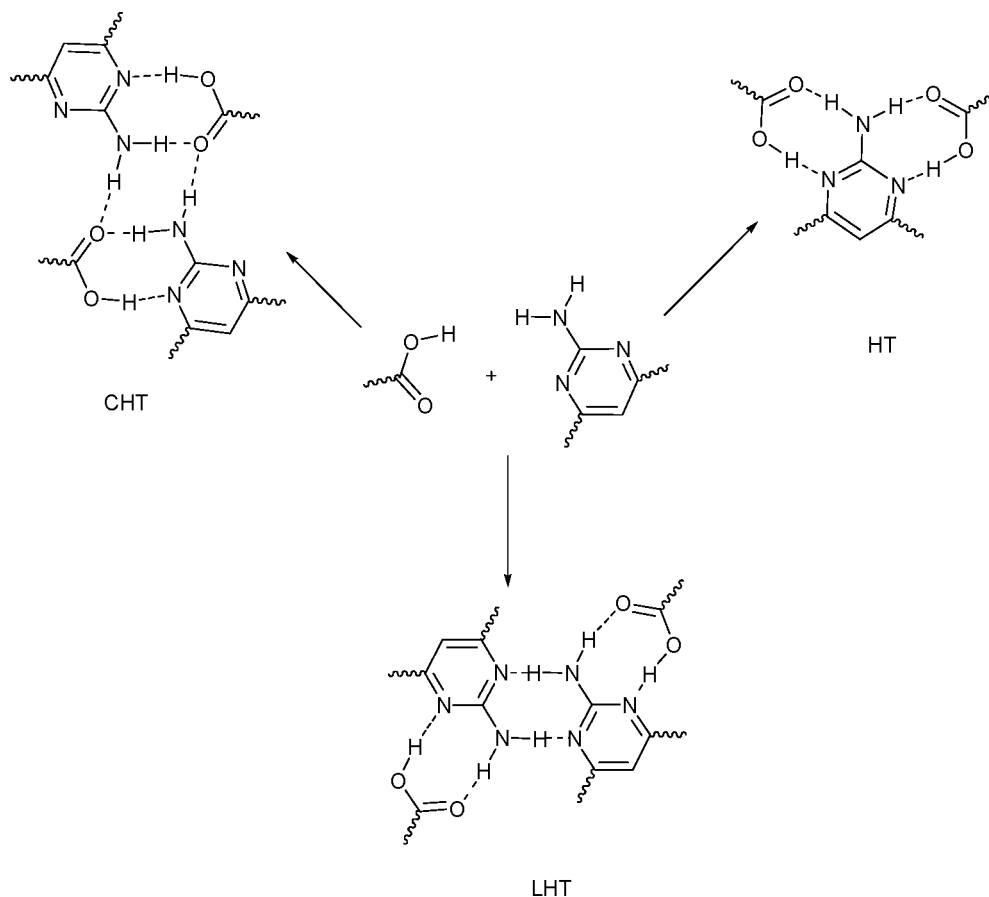
Table 3. Co-crystals/Salts of 2-Amino-4,6-dimethyl Pyrimidine Are Listed in the Increasing Order of ΔpK$_a$, Calculated Using Advanced Chemistry Development Lab Software and SPARC Software, Respectively (Δ pK$_a$ = pK$_a$(base) − pK$_a$(acid))[a]

Advanced Chemistry Development Lab Software					SPARC software				
base (pK$_a$)	acids (pK$_a$)	ΔpK$_a$	salt/co-crystal	ref	base (pK$_a$)	acids (pK$_a$)	ΔpK$_a$	salt/co-crystal	synthons
MP 4.68	2-amino benzoic acid	4.94	−0.26	co-crystal	45	MP 5.24	4-amino benzoic acid	4.75	0.49	co-crystal	LHT
	4-amino benzoic acid	4.86	−0.18	co-crystal	33		adipic acid	4.65	0.59	co-crystal	LHT
	4-hydroxy benzoic acid	4.57	0.11	co-crystal	34		2-amino benzoic acid	4.64	0.6	co-crystal	LHT
	3-benzoyl propionic acid	4.53	0.15	co-crystal	33		glutaric acid	4.51	0.73	co-crystal	LHT
	4-methoxy benzoic acid	4.47	0.21	co-crystal	52		4-methoxy benzoic acid	4.42	0.82	co-crystal	LHT
	3,4-dimethyl benzoic acid	4.44	0.24	co-crystal	52		3 benzoyl propionic acid	4.39	0.85	co-crystal	HT
	adipic acid	4.39	0.29	co-crystal	present		3,4-dimethyl benzoic acid	4.28	0.96	co-crystal	HT
	3,5-dimethyl benzoic acid	4.34	0.34	co-crystal	52		succinic acid	4.27	0.97	co-crystal	HT
	glutaric acid	4.33	0.35	co-crystal	present		3,5-dimethyl benzoic acid	4.18	1.06	co-crystal	HT
	3-methyl benzoic acid	4.27	0.41	co-crystal	53		4-hydroxy benzoic acid	4.17	1.07	co-crystal	others
	succinic acid	4.24	0.44	co-crystal	35		2,4-dimethyl benzoic acid	4.16	1.08	co-crystal	LHT
	benzoic acid	4.20	0.48	co-crystal	52		cinnamic acic	4.11	1.13	co-crystal	HT
	2,4-dimethyl benzoic acid	4.18	0.50	co-crystal	52		2,4,6-trimethyl benzoic acid	4.1	1.14	co-crystal	LHT
	2,5-dimethyl benzoic acid	3.99	0.69	co-crystal	52		3-methyl benzoic acid	4.1	1.14	co-crystal	LHT
	4-chloro benzoic acid	3.97	0.71	co-crystal	53		2,5-dimethyl benzoic acid	4.06	1.18	co-crystal	LHT
	2-methyl benzoic acid	3.95	0.73	co-crystal	53		benzoic acid	4.03	1.21	co-crystal	LHT
	cinnamic acid	3.88	0.80	co-crystal	53		2-methyl benzoic acid	3.98	1.26	co-crystal	LHT
	2,4,6-trimethyl benzoic acid	3.85	0.83	co-crystal	52		4-chloro benzoic acid	3.75	1.49	co-crystal	LHT
	terephthalic acid	3.49	1.19	co-crystal	36		terephthalic acid	3.73	1.51	co-crystal	LHT
	3-nitro benzoic acid	3.48	1.20	co-crystal	53		acetyl salicylic acid	3.63	1.61	co-crystal	LHT
	acetyl salicylic acid	3.48	1.20	co-crystal	52		fumaric acid	3.47	1.77	co-crystal	HT
	4-nitro benzoic acid	3.42	1.26	co-crystal	53		phthalic acid	3.35	1.89	co-crystal	HT
	fumaric acid	3.15	1.53	co-crystal	37		4-nitro benzoic acid	3.21	2.03	co-crystal	LHT
	salicylic acid	3.01	1.67	salt	38		3-nitro benzoic acid	3.19	2.05	co-crystal	LHT
	2-chloro benzoic acid	2.97	1.71	co-crystal	53		2-chloro benzoic acid	3.12	2.12	co-crystal	LHT
	phthalic acid	2.95	1.73	co-crystal	33		salicylic acid	3.08	2.16	salt	LHT
	2,3-difluoro benzoic acid	2.93	1.75	co-crystal	52		malonic acid	2.97	2.27	salt	LHT
	malonic acid	2.92	1.76	salt	present		2,3-difluoro benzoic acid	2.87	2.37	co-crystal	LHT
	3,5-dinitro benzoic acid	2.77	1.91	salt	39		5-chloro salicylic acid	2.65	2.59	salt	CHT
	5-chloro salicylic acid	2.64	2.04	salt	present		3,5-dinitro benzoic acid	2.36	2.88	salt	LHT

[a]In addition to this all the type of synthons formed are also denoted for the corresponding salts and co-crystals.

through discrete heterotetrameric units (combination of three $R_2^2(8)$ motifs).

The next three structures which include **5**, **8**, and **11**, form cyclic heterotetramer through the combination of $R_2^2(8)$, $R_4^2(8)$, and $R_2^2(8)$ motifs. Two of them are co-crystals and one forms a salt. Among these, only **5** and **11** form planar supramolecular sheets.

Structure **6** forms the lone trimer built upon by three $R_2^2(8)$ motifs. This trimer couples with inversely related trimer to form a hexamer, where such hexamer units are interlinked through weak bonds to form infinite ribbons.

One can reason out why structure **10** has not formed one of the expected supermolecule based on the best donor/acceptor guidelines. 3-hydroxy picolinic acid possesses an additional strong donor and acceptor, respectively. The first level of organization in this case is the pyrimidine-carboxylic acid interaction as discussed earlier and differs only in the higher level of supramolecular organization (whether to form a linear heterotetramer, cyclic heterotetramer or a heterotrimer). However in structure **10** after the formation of dimer, the strong acceptor N4 of picolinic acid readily tends to accept a donor N2—H2, amino group of the pyrimidine to form a strong bond in preference to O2 (carboxyl oxygen of the acid molecle) thereby disrupting the formation of a regular cyclic heterotetramer.

The above results in conjunction with the literature survey of co-crystals/salts of MP and MOP shows that 30 out of

Table 4. Co-crystals/Salts of 2-Amino-4,6-dimethoxy Are Listed in the Increasing Order of ΔpK$_a$, Calculated Using Advanced Chemistry Development Lab Software and SPARC Software, respectively (Δ pK$_a$ = pK$_a$(base) − pK$_a$(acid))^a

advanced chemistry development lab software					SPARC software				
base (pK$_a$)	acids (pK$_a$)	ΔpK$_a$	salt/co-crystal	ref	base (pK$_a$)	acids (pK$_a$)	ΔpK$_a$	salt/co-crystal	synthons
MOP 2.93	2-amino benzoic acid	4.94	−2.01	co-crystal	40	MOP 2.85	4-amino benzoic acid	4.75	−1.9	co-crystal	CHT
	4-amino benzoic acid	4.86	−1.93	co-crystal	41		indole-3-acetic acid	4.66	−1.81	co-crystal	others
	4-hydroxy benzoic acid	4.57	−1.64	salt	42		2-amino benzoic acid	4.64	−1.79	co-crystal	LHT
	indole-3-acetic acid	4.49	−1.56	co-crystal	46		4-methoxy benzoic acid	4.42	−1.57	co-crystal	CHT
	4-methoxy benzoic acid	4.47	−1.54	co-crystal	present		succinic acid	4.27	−1.42	co-crystal	CHT
	gallic acid	4.33	−1.4	salt	37		4-hydroxy benzoic acid	4.17	−1.32	salt	LHT
	3-methyl benzoic acid	4.27	−1.34	co-crystal	present		cinnamic acid	4.11	−1.26	co-crystal	LHT
	succinic acid	4.24	−1.31	co-crystal	35		3-methyl benzoic acid	4.1	−1.25	co-crystal	LHT
	cinnamic acid	3.88	−0.95	co-crystal	present		gallic acid	3.98	−1.13	salt	LHT
	4-nitro benzoic acid	3.42	−0.49	co-crystal	present		3-hydroxy picolinic acid	3.87	−1.02	salt	others
	isophthalic acid	3.53	−0.6	co-crystal	present		pyridine-2,6-dicarboxylic acid	3.9	−1.05	salt	CHT
	fumaric acid	3.15	−0.22	salt	37		isophthalic acid	3.72	−0.87	co-crystal	HT
	maleic acid	3.15	−0.22	salt	37		citric acid	3.71	−0.86	salt	others
	tartaric acid	3.07	−0.14	salt	42		fumaric acid	3.47	−0.62	salt	CHT
	salicylic acid	3.01	−0.08	salt	43		maleic acid	3.47	−0.62	salt	others
	2-chloro benzoic acid	2.97	−0.04	co-crystal	present		phthalic acid	3.35	−0.5	co-crystal	HT
	pyridine-2,6-dicarboxylic acid	2.97	−0.04	salt	42		4-nitro benzoic acid	3.21	−0.36	co-crystal	LHT
	phthalic acid	2.95	−0.02	co-crystal	44		tartaric acid	3.16	−0.31	salt	others
	citric acid	2.93	0	salt	37		2-chloror benzoic acid	3.12	−0.27	co-crystal	LHT
	2,4-dichloro benzoic acid	2.68	0.25	co-crystal	37		salicylic acid	3.08	−0.23	salt	CHT
	chloro acetic acid	2.65	0.28	co-crystal	present		chloroacetic acid	2.97	−0.12	co-crystal	LHT
	5-chloro salicylic acid	2.64	0.29	salt	present		2,4-dichlro benzoic acid	2.83	0.02	co-crystal	CHT
	3-hydroxy picolinic acid	1.14	1.79	salt	present		5-chloro salicylic acid	2.65	0.2	salt	LHT
	trichloro acetic acid.	0.09	2.84	salt	present		trichloroacetic acid	0.66	2.19	salt	CHT

^{a}In addition to this all the type of synthons formed are also denoted for the corresponding salts and co-crystals. LHT = linear heterotetramer, CHT = cyclic heterotetramer, and HT= heterotrimer.

54 (around 56%) leads to the formation of linear heerotetramer synthon, 9 of them form cyclic heterotetramers (around 17%), 9 others form heterotrimers (around 17%) and the rest form other new synthons (around 11%). This clearly states that the linear heterotetramer synthon is the most predominantly existing synthon. It is also predicted to be the most stable one formed when an aminopyrimidine and carboxylic acid interact with each other which is exemplified by a crystal structure prediction study carried out by Thakur and Desiraju.[52] In fact one of our recently published work also clearly demonstrates that this stable linear heterotetrameric synthon is responsible for the formation several isostructural co-crystals.[53]

The present work has produced a list of multicomponent crystals which include salts and co-crystals. It is well-known that when an acid crystallizes with a base it either forms a salt or co-crystal (Scheme 4). The rationalization to the formation of these salts/co-crystals involving MOP and MP with various acids has also been attempted to explain in terms of pK$_a$ values. Among the 14 structures, 9 of them are co-crystals while the remaining are

salts. From the literature it is clear that the acid dissociation constant, pK$_a$ have been used quite successfully in predicting and rationalizing the formation of salts/co-crystals. We have tried to reason the observed structural behavior through a comparative analysis of the calculated pK$_a$ values for all the structures. The two pyrimidine derivatives are basic compounds with calculated pK$_a$ values of 4.68 (5.24) and 2.93 (2.85) respectively.[54,56] Molecular complexes of these pyrimidines with various carboxylic acids (present work and the reported structures) in the increasing order of pK$_a$ are presented in Table 3 and Table 4.

The C−N−C bond angle in MOP and MP, which involves acid−base interaction range from 115 to 118° in most cases (indicative of co-crystal fomation) and increases to a higher range of 120−122° indicating the formation of salts. This is supported by the C−O bond distances determined through X-ray crystallographic study. A plot for all the structures including those in the literature, with X-axis corresponding to the ΔpK$_a$ [where ΔpK$_a$ = pK$_a$(base) − pK$_a$(acid)] and Y-axis corresponding to ΔD$_{C−O}$
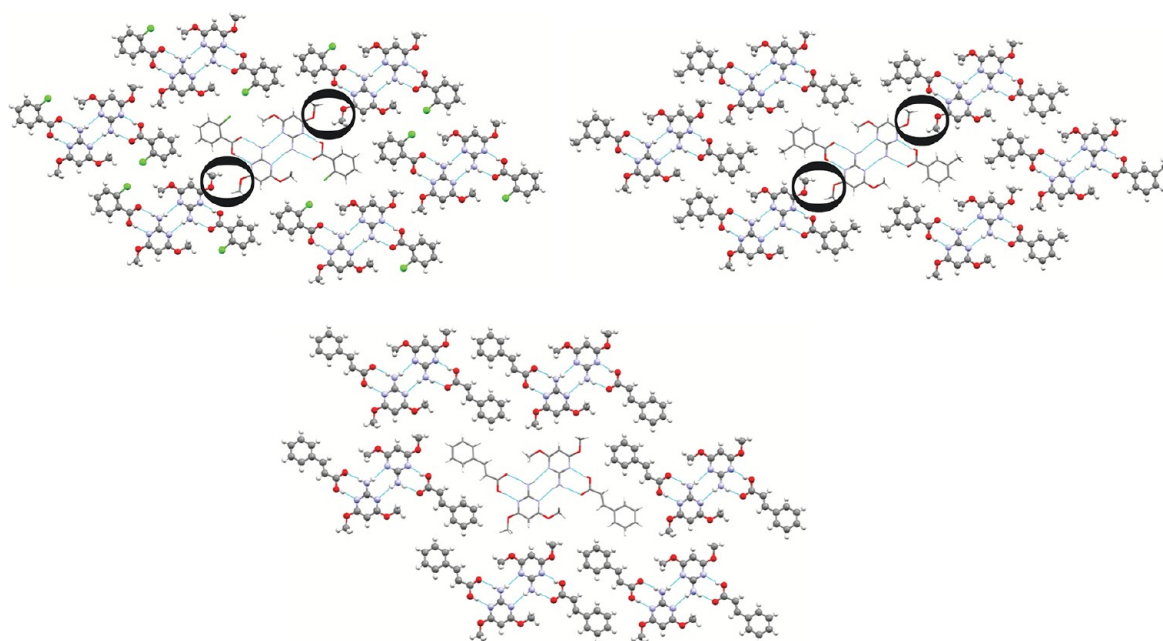
Figure 23. View of a supramolecular sheet formed in **1**, **2**, and **3** where each tetramer is surrounded by six adjacent tetramers. The ellipses denote the formation of $R_2^2(6)$ synthon between adjacent methoxy groups in **1** and **2**.

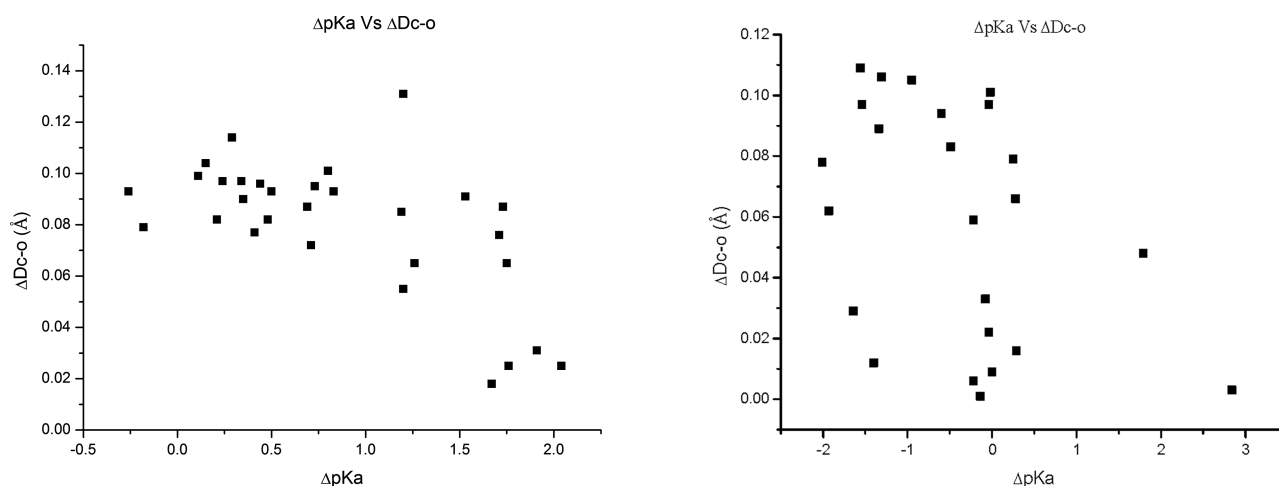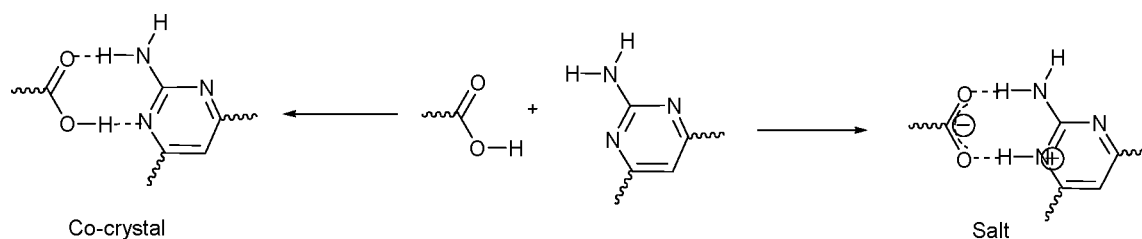**Scheme 4. Scheme Combination of Acid and Base to Give Either a Co-crystal or Salt**

Figure 24. Plot of ΔpK_a vs $\Delta Dc\text{-}o$ for all the MP (left) and MOP (right) co-crystals/salts with various carboxylic acids.

(difference between the lengths of the two C−O bonds in a carboxyl group) bond lengths, is shown in Figure 24. The scattergram indicates that the densely populated top left corner corresponds to co-crystals having larger ΔD_{C-O} and the scarcely populated bottom right corner to formation of salts. It is observable that for MP there is some low negative corelation whereas for MOP the regularity has been unseen and no correlation. A similar plot has been reported in the literature.[57]

Even if the usefulness of pK_a values is dubious in the ability to predict the formation of co-crystals/salts, the approach has made possible to identify the occurrence of proton transfer atleast before the actual experiment has been carried out. Several papers have reported the use of pK_a to predict salt/co-crystals.[57−55] It has been identified that the reliability and the applicability have been uncertain when the ΔpK_a ranges between 0 and 3. It is expected that salt formation is predominant when ΔpK_a is

greater than 3, and likewise they correctly form co-crystals when the ΔpK_a is negative. There is poor predictive power between the range of 0 to 3,[57] and this narrow continuum differs for different system. Infact we have tried to identify the narrow continuum that exists for our system containing two aminopyrimidine bases.

The ΔpK_a calculated using Advanced Chemistry Development Software[54] shows good agreement with the results obtained with only few exceptions, which is likely when a large set of data is analyzed (Table 3). The narrow transition where the salts and co-crystals overlap with each other is between ΔpK_a 1.50 and 1.75 in the case of MP. In order to cross-check whether the theoretical calculations performed were reliable, the same sets of calculations were performed with another software named SPARC.[56] The results substantiated the earlier results qualitatively but failed quantitatively. The change in pK_a from 4.68 (MP) to 2.93 (MOP) is expected to form more number of co-crystals, in contrast the percentage of co-crystals formed are 88% and 52% for MP and MOP respectively. It is also evident that the pK_a of MOP does not clearly predict the formation of co-crystals despite the fact that ΔpK_a values for majority of the complexes lie below zero leading to some ambiguity (Table 4). Not all systems that are considered strictly follow the pK_a guidelines. The results do not show the expected outcome which could be due to several factors such as the environment of the crystal structure, methods of reaction conditions used in the preparation of the complexes, nature of solvents and even the unreliable theoretical values of pK_a used in the calculation.

■ CONCLUSION

This systematic study reveals that the complementary pair of O—H···N/O⁻···H—N⁺ and N—H···O⁻/N—H···O hydrogen bonds in the family of MOP/MP- carboxylic acids readily assemble to form $R_2^2(8)$ motif which further self-assembles to aid in building a larger supermolecule - LHT, CHT, HT and others. Since 56% of the structures form the LHT, the high supramolecular yield implicates the reliability of this synthon.

In the absence of other strong functional groups in the aromatic ring, it is the weak C—H···O, Cl···Cl, and stacking interactions that determine the overall arrangement of the tetramers. Therefore the heterotetrameric synthons can be used extensively for the construction of larger supramolecular architectures by substituting suitable functional groups in the aromatic acid with the knowledge on the hierarchy of hydrogen bonds.

Apart from all these synthons, a new $R_2^2(6)$ motif, formed primarily between a couple of inversely related methoxy group seems to be frequently occurring in our study. Although in most cases this is far from the range of the regular C—H···O bond lengths, a thorough investigation could provide some insight into this new synthon. Structures **1**, **2**, and **10** show this type of synthons.

The above results and the synthetic strategies can also be employed practically to other biological relavant systems.

On the basis of molecular co-crystals/salts presented here as well as those reported from literature, the ΔpK_a clearly demonstrates that MP is a good co-crystal former when combined with carboxylic acids in contrast to MOP, which is of unpredictive nature.

■ ASSOCIATED CONTENT

Ⓢ Supporting Information

Crystallographic information files (CIF) of structures **1−14**. This material is available free of charge via the Internet at http://pubs.acs.org.

■ AUTHOR INFORMATION

Corresponding Author

*E-mail: tommtrichy@yahoo.co.in Phone: ++91-431-2407053 Fax: ++91-431-2407045, 2407030.

Notes

The authors declare no competing financial interest.

■ ACKNOWLEDGMENTS

■ REFERENCES

(1) Legon, A. C.; Millen, D. J. In *Principles of Molecular Recognition*; Buckingham, A. D., Legon, A. C., Roberts, S. M., Eds.; Blackie Academic and Professional: London, 1993.

(2) von Hippel, P. H.; Berg, O. G. *Proc. Natl. Acad. Sci. U. S. A.* **1986**, *83*, 1608−1612.

(3) Hippel, P. H. V. ; Berg, O. G. In *DNA-Ligand Interactions*; Plenum Publishing Corp.: New York, 1987.

(4) Sundberg, E. J.; Mariuzza, R. A. *Adv. Protein Chem.* **2002**, *61*, 119−160.

(5) Weis, W. I. *Annu. Rev. Biochem.* **1996**, *65*, 441−473.

(6) Ofek, I.; Sharon, N. *Infect. Immun.* **1988**, *56*, 539−547.

(7) Lehn, J. M. *Supramolecular Chemistry: Concepts and Perspectives*; VCH: Weinheim, Germany, 1995.

(8) Atwood, J. L.; Davies, J. E. D.; MacNicol, D. D.; Vögtle, F. In *Comprehensive Supramolecular Chemistry*; Lehn, J.-M., Ed.; Pergamon: Oxford, U.K., 1996.

(9) Aakeroy, C. B.; Beatty, A. M. *Aust. J. Chem.* **2001**, *54*, 409−421.

(10) Steiner, T. *Angew. Chem., Int. Ed.* **2002**, *41*, 48−76.

(11) Bernstein, J.; Davis, R. E.; Shimoni, L.; Chang, N. L. *Angew. Chem., Int. Ed. Engl.* **1995**, *34*, 1555−1573.

(12) Kollman, P. A. *J. Am. Chem. Soc.* **1972**, *94*, 1837−1842.

(13) Aakeroy, C. B.; Seddon, K. R. *Chem. Soc. Rev.* **1993**, *22*, 397−407.

(14) Walsh, R. D. B.; Bradner, M. W.; Fleischman, S.; Morales, L. A.; Moulton, B.; Rodriguez-Hornedo, N.; Zaworotko, M. J. *Chem. Commun.* **2003**, 186−187.

(15) Bis, J. A.; Zaworotko, M. J. *Cryst. Growth Des.* **2005**, *5*, 1169−1179.

(16) Vishweshwar, P.; Nangia, A.; Lynch, V. M. *Cryst. Growth Des.* **2003**, *3*, 783−790.

(17) Aakeroy, C. B.; Beatty, A. M.; Helfrich, B. A. *J. Am. Chem. Soc.* **2002**, *124*, 14425−14432.

(18) Bhogala, B. R.; Vishweshwar, P.; Nangia, A. *Cryst. Growth Des.* **2002**, *2*, 325−328.

(19) Fleischman, S. G.; Kuduva, S. S.; Mcmahon, J. A.; Moulton, B.; Walsh, R. D. B.; Rodriguez-Hornedo, N.; Zaworotko, M. J. *Cryst. Growth Des.* **2003**, *3*, 909−919.

(20) Reddy, L. S.; Nangia, A.; Lynch, V. M. *Cryst. Growth Des.* **2004**, *4*, 89−94.

(21) Vangala, V. R.; Mondal, R.; Broder, C. K.; Howard, J. A. K.; Desiraju, G. R. *Cryst. Growth Des.* **2005**, *5*, 99−104.

(22) Allen, F. H.; Raithby, P. R.; Shields, G. P.; Taylor, R. *Chem. Commun.* **1998**, 1043−1044.

(23) Allen, F. H.; Motherwell, W. D. S.; Raithby, P. R.; Shields, G. P.; Taylor, R. *New J. Chem.* **1999**, 25−34.

(24) Jeffrey, G. A.; Saenger, W. *Hydrogen Bonding in Biological Structures*; Springer-Verlag: Berlin, 1991.

(25) Schmidt, L. H.; Harrison, J.; Rossan, R. N.; Vaughan, D.; Crosby, R. *Am. J. Trop. Med. Hyg.* **1977**, *26*, 837−849.

(26) Vallee, B. L.; Auld, D. S. *Acc. Chem. Res.* **1993**, *26*, 543−551.

(27) Hunt, W. E.; Schwalbe, C. H.; Bird, K.; Mallinson, P. D. *J. Biochem.* **1980**, *187*, 533−536.

(28) Baker, B. R.; Santi, D. V. *J. Pharm. Sci.* **1965**, *54*, 1252−1257.

(29) Serajuddin, A. T. M. *Adv. Drug Delivery Rev.* **2007**, *59*, 603−616.

(30) Blagden, N.; de Matas, M.; Gavan, P. T.; York, P. *Adv. Drug Delivery Rev.* **2007**, *59*, 617−630.

(31) Reddy, L. S.; Bethune, S. J.; Kampf, J. W.; Hornedo, N. R. *Cryst. Growth Des.* **2009**, *9*, 378−385.

(32) Stanton, M. K.; Tufekcic, S.; Morgan, C.; Bak, A. *Crystal Cryst. Growth Des.* **2009**, *9*, 1344−1352.

(33) Balasubramani, K. Ph.D. Thesis, School of Chemistry, Bharathidasan University, 2007.

(34) Balasubramani, K.; Muthiah, P. T.; Lynch, D. E. *Acta Crystallogr.* **2006**, *E62*, o2907−o2909.

(35) Devi, P. Ph.D. Thesis, School of Chemistry, Bharathidasan University, 2009.

(36) Devi, P.; Muthiah, P. T. *Acta Crystallogr.* **2007**, *E63*, o4822−o4823.

(37) Thanigaimani, K. Ph.D. Thesis, Bharathidasan University, 2009.

(38) Muthiah, P. T.; Balasubramani, K.; Rychlewska, U.; Plutecka, A. *Acta Crystallogr.* **2006**, *C62*, o605−o607.

(39) Subashini, A.; Muthiah, P. T.; Lynch, D. E. *Acta Crystallogr.* **2008**, *E64*, o426.

(40) Thanigaimani, K.; Muthiah, P. T.; Lynch, D. E. *Acta Crystallogr.* **2008**, *E64*, o107−o108.

(41) Thanigaimani, K.; Muthiah, P. T.; Lynch, D. E. *Acta Crystallogr.* **2006**, *E62*, o2976−o2978.

(42) Thanigaimani, K.; Muthiah, P. T.; Lynch, D. E. *Acta Crystallogr.* **2007**, *C63*, o295−o300.

(43) Thanigaimani, K.; Muthiah, P. T.; Lynch, D. E. *Acta Crystallogr.* **2007**, *E63*, o4555−o4555.

(44) Thanigaimani, K.; Muthiah, P. T.; Lynch, D. E. *Acta Crystallogr.* **2007**, *E63*, o4212.

(45) Ebenezer, S.; Muthiah, P. T. *Acta Crystallogr.* **2010**, *E66*, o516.

(46) Ebenezer, S.; Muthiah, P. T. *Acta Crystallogr.* **2010**, *E66*, o2634−o2635.

(47) Bruker. *SMART APEX2, SAINT, and SADABS*; Bruker AXS Inc.: Madison, WI, U.S.A., 2008.

(48) Sheldrick, G. M. *Acta Crystallogr. A.* **2008**, *64*, 112−122.

(49) Spek, A. L. *J. Appl. Crystallogr.* **2003**, *36*, 7−13.

(50) Macrae, C. F.; Bruno, I. J.; Chisholm, J. A.; Edgington, P. R.; McCabe, P.; Pidcock, E.; Rodriguez-Monge, L.; Taylor, R.; Streek, J. V. D.; Wood, P. A. *J. Appl. Crystallogr.* **2008**, *41*, 466−470.

(51) Desiraju, G. R. *Angew. Chem., Int. Ed. Engl.* **2003**, *34*, 2311−2327.

(52) Thakur, T. S.; Desiraju, G. R. *Cryst. Growth Des.* **2008**, *8*, 4031.

(53) Ebenezer, S.; Muthiah, P. T.; Butcher, R. *J. Cryst. Growth Des.* **2011**, *11*, 3579−3592.

(54) Calculated using Advanced Chemistry Development (ACD/Labs) Software V 8.00 for Microsoft windows (1994−2009 ACD/Labs)

(55) Hilal, S. H.; Karickhoff, S. W.; Carreira, L. A. *Quant. Struc. Act. Rel* **1995**, *14*, 348−355.

(56) Childs, S. L.; Stahly, G. P.; Park, A. *Mol. Pharmaceutics* **2007**, *4*, 323−338.

(57) Aakeröy, C. B.; Desper, J.; Urbina, J. F. *Chem. Commun.* **2005**, 2820−2822.

(58) Aakeröy, C. B.; Desper, J.; Scott, B. M. T. *Chem. Commun.* **2006**, 1445−1447.

(59) Aakeröy, C. B.; Beatty, A. M.; Helfrich, B. A. *Angew. Chem., Int. Ed.* **2001**, *40*, 3240−3242.

(60) Lynch, D. E.; McClenaghan, I. *Acta Crystallogr.* **2001**, *C57*, 830−832.